Joint Impacts of Imperfect CSI and Imperfect SIC in Cognitive Radio-Assisted NOMA-V2X Communications

DINH-THUAN DO[ID][1]**, (Senior Member, IEEE), TU ANH LE**[ID][2]**,**
TU N. NGUYEN[ID][3]**, (Senior Member, IEEE), XINGWANG LI**[ID][4,5]**, (Senior Member, IEEE),**
AND KHALED M. RABIE[ID][5]**, (Senior Member, IEEE)**

[1]Wireless Communications Research Group, Faculty of Electrical & Electronics Engineering, Ton Duc Thang University, Ho Chi Minh City 700000, Vietnam
[2]Faculty of Electronics Technology, Industrial University of Ho Chi Minh City, Ho Chi Minh City 700000, Vietnam
[3]Department of Computer Science, Purdue University Fort Wayne, Fort Wayne, IN 46805, USA
[4]School of Physical and Electronics Engineering, Henan Polytechnic University, Jiaozuo 454000, China
[5]Department of Engineering, Manchester Metropolitan University, Manchester M1 5GD, U.K.

Corresponding authors: Dinh-Thuan Do (dodinhthuan@tdtu.edu.vn) and Khaled M. Rabie (k.rabie@mmu.ac.uk)

ABSTRACT In this study, the performance of a secondary network in cognitive radio (CR) is studied in the context of vehicle-to-everything (V2X). The non-orthogonal multiple access (NOMA) is effectively applied in this new system model, namely CR-assisted NOMA-V2X, and it is beneficial to serve group of vehicles. In our proposed system, two schemes related to vehicle-to-vehicle (V2V) transmissions are further considered to enhance performance of the vehicle that needs higher quality of service (QoS). However, the degradation performance can be predicted by evaluating downlink under impacts from interference from the primary network, imperfect channel state information (CSI) and imperfect successive interference cancellation (SIC). The outage performance gap among two vehicles exists since different power allocation factors were assigned to them. To validate the system performance, the outage probability is first derived in exact and approximate forms and then the throughput can be further achieved. The optimal throughput can be obtained by numerical simulations. Simulation results are provided to verify the correctness of the derived expressions and it exhibits advantages of the proposed CR-assisted NOMA-V2X system in terms of outage probability and the throughput.

INDEX TERMS Vehicle-to-everything, cognitive radio, non-orthogonal multiple access, imperfect CSI.

I. INTRODUCTION

Recently, vehicle-to-everything (V2X) communications has introduced to provide more advantages for vehicular networks including more efficient, smarter, and safer road traffic [1]. There are several types of V2X communications such as vehicle-to-vehicle (V2V), vehicle-to-infrastructure (V2I) and vehicle-to-pedestrian (V2P). In potential scenarios, V2X is designed to support real-time traffic information transmission among infrastructure, vehicles and pedestrians [2], [3]. Vehicular networks with signal processing techniques in 5G wireless systems are developed to guarantee reliability and safety of vehicles. Therefore, great efforts in standards and projects related to vehicular communications

The associate editor coordinating the review of this manuscript and approving it for publication was Javed Iqbal[ID].

have been reported, for example the European Union Mobile and wireless communications Enablers for Twentytwenty Information Society (METIS) project, IEEE 802.11p, and the third generation partnership project (3GPP) long term evolution vehicle (LTE-V) [4]. The fast growth of the number of connected vehicles in vehicular networks results in challenges associated with quality of V2X communications such as low access efficiency and severe data congestion.

Since the orthogonal multiple access (OMA) employed in the existing LTE networks, the dense networks meet difficulties such as the limited spectrum resources, severe data congestion and low access efficiency. Therefore, developing 5G wireless network in V2X scheme requires a more efficient radio access technology. Fortunately, non-orthogonal multiple access (NOMA) has recently considered to incooperate with the V2X [5]. NOMA brings to V2X some benefits since

it exploits power domain to signal multiplexing at the transmitter side and performs superposed coding (SC) at receiver side [6]–[11]. As main advantages, NOMA is proved with good characterizations including higher reliability, higher transmission rates, lower system latency and lower-cost service requirements in comparison with the traditional OMA method [12]. By combining NOMA and V2X, NOMA-V2X is considered as promising scheme to mitigate resource collision, and hence enhancing the spectrum efficiency and reducing the latency [13]. The authors in [14] presented two relay-assisted NOMA transmission architectures for V2X communications including half-duplex relay-assisted NOMA and full-duplex relay-assisted NOMA. Regarding full duplex NOMA based decentralized V2X system model, the capacity performance improvement can be achieved by increasing the number of V2X devices, transmit power, and Rician factor value [15]. The authors in [16] proposed a power control scheme for NOMA-V2X to balance the power allocation among the selected cluster-head vehicles to further improve the throughput in downlink.

In other trends of application of NOMA, it can be combined with cognitive radio (CR) which is also examined as a promising technique to improve the spectrum efficiency by allocating the secondary vehicles to dynamically access the licensed spectrum [17]. Such advantage of CR is extended with NOMA to introduce new system of CR-NOMA [18]–[25]. For example, a cooperative NOMA system was studied with imperfect successive interference cancellation (SIC) to highlight the performance of an underlay CR networks [18]. The authors in [19] discussed security and reliability performance of cooperative NOMA in the context of CR. In such CR-NOMA, the confidential messages are sent by both a NOMA-strong primary vehicle (PU) and a primary base station (PBS) to multiple uniformly distributed primary vehicles in the scenario of randomly situated surrounding eavesdroppers. The recent work in [20] provided a new system model in which the secondary vehicles are able to harvest energy from the radio-frequency signals to securely transmit the secondary secure messages by employing NOMA. There are three main metrics including connection outage probability, secrecy outage probability, and effective secrecy throughput studied analytically to examine the performance of the primary vehicles over Nakagami-m fading channels in which eavesdroppers are the secondary vehicles [21]. In [22], the authors analyzed resource allocation schemes for cognitive heterogeneous network (Hetnet) under interweave spectrum sharing mode and such Hetnet implements in two-tier. It was shown that the spectral efficiency can be significantly improved by using NOMA in the CR compared to that achieved by using OMA in CR. The underlay and/or overlay spectrum sharing strategies are widely implemented in the current researches about the CR networks. The authors in [25] proposed CR-NOMA and it is particularly useful when the secondary source has good channel conditions to a primary receiver but lacks the radio spectrum. Such model of spectrum-sharing CR network was

evaluated in terms of outage probability and system throughput.

Most previous works regarding NOMA systems above assumed perfect channel state information (CSI). However, in real conditions, a NOMA network needs to be investigated in practical case of imperfect CSI [26], [27]. The authors in [27] examined beamforming vectors and the power allocation to maximize the system utility of multiple-input multiple-output NOMA (MIMO-NOMA) with respect to probabilistic constraints. The interesting solution is described that introducing first-order approximation and semidefinite programming (SDP) to form an efficient successive convex approximation (SCA) scheme. Several multiplexed vehicles can be proceeded in a NOMA transmission and the imperfect CSI needs to be considered in term of resource allocation as in [28]. The metrics including outage probability and system throughput for the primary and secondary networks (SNs) are derived and hence it demonstrates the superior performance compared with conventional OMA [25]. They were also compared with system performance benchmark by exploiting optimal vehicle scheduling based on exhaustive search [28].

In order to improve the spectral efficiency in the situation of several vehicles located in close distance, device-to-device (D2D) is proposed to enhance system performance. Such D2D transmission would be beneficial if D2D is combined with existing NOMA scheme [32]. Then, considering a cluster which contains a D2D pair and two cellular vehicles, the power control scheme is necessary in design of the base station (BS). More specifically, BS permits cellular vehicles to achieve a higher sum rate and higher individual rates in NOMA compared to OMA, and the related evaluations were reported in [33]. By jointly optimizing the vehicle clustering and power assignment, the authors in [34] presented optimal sum-rate of the network. Moreover, the authors also aim to exhibit interference protection for the cellular vehicles. Their main result indicated that the proposed algorithm can achieve up to 70 percentage and 92 percentage of performance gains in terms of the average sum-rate in comparison with the general NOMA and traditional orthogonal frequency-division multiple access (OFDMA) system, respectively.

A. OUR CONTRIBUTION

It is worth pointing out that few papers studied CR-assisted NOMA-V2X. In fact, problem of performance improvement for vehicles in the secondary network (SN) of CR-assisted NOMA-V2X has not been studied well. Motivated by [5], [31], this paper considers CR-assisted NOMA-V2X system using Nakagami-m fading channels. More importantly, it is necessary to understand the challenges and benefits of V2V transmissions under impacts of imperfect CSI and interference from cellular vehicles (CUE). As a main goal, we analyze the outage probability and throughput performance of the CR-assisted NOMA-V2X system enabling V2V (D2D) links. We derive the closed-form expressions of the outage probability at each vehicle. Furthermore, joint impact of imperfect SIC and imperfect CSI on such networks need

to be exploited to indicate the performance gap among two vehicles. By studying analytical performance analysis, detail guidelines are provided for deploying such CR-assisted NOMA-V2X.

The following is a summary of the main contributions of this study:

- Reliable transmission is achieved as employing V2V in the SN of CR-assisted NOMA-V2X system over Nakagami-*m* fading channel with interference constraint. We intend to analyze the system performance under imperfect SIC and imperfect CSI.
- This implementation in CR-assisted NOMA-V2X is necessary to evaluate the performance gap among two vehicles. Especially, we study two schemes corresponding with and without V2V links. In this scenario, we assumed that two vehicles are classified into non-SIC and SIC user. When V2V link is used (Scheme I), it can provide better outage performance compared with Scheme II which does not require V2V link.
- Both exact and approximate expressions of outage probability are derived and then throughput is further examined. From the achieved results, we analyze the effects of a number of factors including power allocation factors, transmit SNR, and CSI imperfection levels to prove the superiority of the considered NOMA-V2X model.
- Moreover, these findings are verified by simulations to highlight advantages of the CR-assisted NOMA-V2X system. The obtained results indicate that status of SIC, target rates, and power allocation factors are main impacts on performance of such systems in terms of outage probability and throughput.

B. ORGANIZATION

The remaining sections are organized as follows. Section II describes the system model of CR-assisted NOMA-V2X. Section III analyzes the outage probability in the case of V2V link so-called as Scheme I. Section IV presents the outage performance of two vehicles in Scheme II. The throughput and asymptotic performance are presented in V. Section VI presents numerical results and simulation examples. The conclusion is presented in Section VII.

II. SYSTEM MODEL AND SIGNAL PROCESSING CONSIDERATION

The considered system model of NOMA-V2X in the context of CR network is shown in Fig. 1. As main characterization of such NOMA-V2X, the system comprises primary network (PN) and underlay SN which is able to operate under interference constraint. The V2V link is employed at SN to perform communication in close distance while the main links from the BS serves pair of vehicles (V_1, V_2). Here, the BS plays a role as Roadside Unit (RSU) in the context of V2X communication [14]. Operating together with PN, the SN meets interference from primary transmitter (PT) which belongs to the PN [31]. Three vehicles in the SN also make impacts on the primary vehicle (PV) in the PN, with
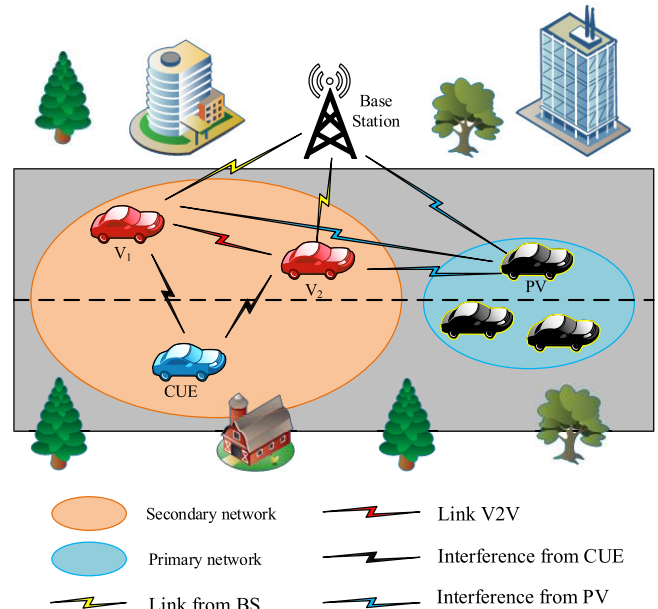

FIGURE 1. System model of the secondary network in considered CR-assisted NOMA-V2X system.

denotations: h_{SP}, h_{1P}, h_{2P} the channel gains for the links as PV to BS, V_1 and V_2 respectively. The channel gains are denoted as h_1 and h_2 for link from the BS to the first vehicle, the second vehicle respectively. Regarding interference between CUE and vehicles in the SN, I_P denotes the fixed interference term. While $h_{k,i}$ is channel serving V2V transmission ($i, k \in \{1; 2\}$ and $i \neq k$). The channel u represents exponential distribution with means λ_u.

In this study, it is assumed that the CSI related channels are estimated imperfectly at the receivers, it is given by [26], [27]

$$h_j = \hat{h}_j + e_j, \tag{1}$$

where $j \in \{i; SP; iP; k, i\}$, $\hat{h}_j$ illustrates the estimated channel factor $\hat{h}_j \sim CN(0, \lambda_j)$, e_j represent the channel estimation error with $e_j \sim CN(0, \lambda_{e_j})$. The noise terms in each receiver is assumed as Additive White Gaussian Noise (AWGN) with a variance of N_0. Moreover, $I_P \sim CN(0, N_0\mu)$, μ indicates the level of interference and CSI of primary transmitters is not available at the secondary receivers [31]. Thus, the power of the secondary transmitter vehicle Q is restricted as $P_Q \leq \min\left(\frac{I_{th}}{|h_l|^2}, \bar{P}_S\right)$, $Q \in \{S, V_i\}$ and $l \in \{SP, iP\}$, where $\bar{P}_Q$ denotes the maximum average allowed transmit power while I_{th} denotes as the interference temperature constraint (ITC) at the vehicle PV [31].

Adopting the NOMA-V2X model developed in [14], x_1 and x_2 are denoted as the messages sent by the BS which serves both the weak vehicle V_1 (located at far distance) and the strong vehicle V_2 (placed at near distance compared with the BS). Regarding power percentage for each vehicle, α_1 and α_2 use to denote as the power allocation coefficients for V_1

and V_2 in NOMA, respectively. Following the principle of NOMA, it can be assumed that $\alpha_1 > \alpha_2$ with $\alpha_1 + \alpha_2 = 1$.[1]

In the first phase, due to imperfect CSI at the vehicle, the received signal at the vehicle V_i is expressed by

$$
\begin{aligned}
y_i &= \left(\hat{h}_i + e_i\right)\sqrt{P_S}\left(\sqrt{\alpha_1}x_1 + \sqrt{\alpha_2}x_2\right) + I_P + n_i \\
&= \hat{h}_i\sqrt{P_S}\left(\sqrt{\alpha_1}x_1 + \sqrt{\alpha_2}x_2\right) \\
&\quad + e_i\sqrt{P_S}\left(\sqrt{\alpha_1}x_1 + \sqrt{\alpha_2}x_2\right) + I_P + n_i,
\end{aligned}
\tag{2}
$$

where n_i is denoted as the AWGN with variance N_0. Regarding the signal detection at receiver, the signal-to-interference-plus-noise ratio (SINR) need to be calculated to further achieve other performance evaluations. Such SINR after detecting x_1 at V_1 can be computed as

$$
\gamma_{V_1 \to x_1} = \frac{\left|\hat{h}_1\right|^2 \alpha_1 \rho_S}{\left|\hat{h}_1\right|^2 \alpha_2 \rho_S + \rho_S |e_1|^2 + \bar{\mu}},
\tag{3}
$$

where $\bar{\mu} = \mu + 1$ and $\rho_S = \frac{P_S}{N_0}$ is the transmit SNR at the BS. Similarly, the SINR to decode x_1 at V_2 is expressed by

$$
\gamma_{V_2 \to x_1} = \frac{\left|\hat{h}_2\right|^2 \alpha_1 \rho_S}{\left|\hat{h}_2\right|^2 \alpha_2 \rho_S + \rho_S |e_2|^2 + \bar{\mu}}.
\tag{4}
$$

To implement NOMA, by performing SIC, SINR to detect signal x_2 at V_2 can be given by

$$
\gamma_{V_2 \to x_2} = \frac{\left|\hat{h}_2\right|^2 \alpha_2 \rho_S}{\rho_S |e_2|^2 + \bar{\mu}}.
\tag{5}
$$

Now, we look at the V2V link for Scheme I,[2] x_c is signal communicating via the V2V link, then the received signal at V_i ($i = 1, 2$) can be given as

$$
c_i = \hat{h}_{k,i} P_{V_i} x_c + e_{k,i} P_{V_i} x_c + I_P + n_{c,i}.
\tag{6}
$$

Here, x_c and x_1 are unit signals with $E\left\{|x_1|^2\right\} = E\left\{|x_c|^2\right\} = 1$ where $E(.)$ is the expectation operation. In next step, signal to noise ratio (SNR) can be obtained to decode signal at each vehicle corresponding to V2V link as

$$
W_i = \frac{\rho_{V_i}\left|\hat{h}_{k,i}\right|^2}{\rho_{V_i}\left|e_{k,i}\right|^2 + \bar{\mu}},
\tag{7}
$$

where $\rho_{V_i} = \frac{P_{V_i}}{N_0}$ is the SNR at the corresponding destination. In the final step, the SINR for decoding x_1 under the combination of V2V link and downlink NOMA from the BS

is formulated as

$$
\begin{aligned}
&Z_{V2V} \\
&= \begin{cases} \min(\max\{\gamma_{V_1 \to x_1}, W_1\}, \gamma_{V_2 \to x_1}) & \text{if:} |\hat{h}_1|^2 < |\hat{h}_2|^2 \\ \min(\max\{\gamma_{V_2 \to x_1}, W_2\}, \gamma_{V_1 \to x_1}), & \text{otherwise.} \end{cases}
\end{aligned}
\tag{8}
$$

In the next section, we further evaluate outage performance metric based on SINR achieved in this section.

A. CHANNEL MODEL

In order to model cooperative vehicular communication and short-range communications, the Nakagami-m fading channel model is widely implemented.[3] Based on this, the probability density function (PDF) and the cumulative distribution function (CDF) of channel h_j respectively

$$
f_{|h_j|^2}(x) = \frac{x^{m_j - 1} e^{-\frac{x}{\Omega_j}}}{\Gamma(m_j)\Omega_j^{m_j}},
\tag{9}
$$

and

$$
F_{|h_j|^2}(x) = 1 - \frac{\Gamma(m_j, x/\Omega_j)}{\Gamma(m_j)},
\tag{10}
$$

where $\Omega_j = \frac{\lambda_j}{m_j}$ and, m_j and λ_j represent the fading severity factor and mean, respectively. $\Gamma(.)$ is the upper incomplete Gamma function which is defined in [36, 8.350]. In this paper, it is also assumed that m_j is an integer number, $m_j \geqslant 1$ and $\Gamma(n) = (n-1)!$. Moreover, $F_{|h_j|^2}(x)$ can be expressed as

$$
F_{|h_j|^2}(x) = 1 - e^{-\frac{x}{\Omega_j}} \sum_{i=0}^{m_j - 1} \frac{x^i}{\Omega_j^i i!}.
\tag{11}
$$

III. SCHEME I: NOMA-V2X WITH V2V LINK
A. OUTAGE PROBABILITY OF THE FIRST VEHICLE

In this subsection, this paper investigates the outage performance of each destination in term of the outage probability. To be more specific, such outage metric quantifies the probability that the message which cannot be decoded at the intended receiver without error [37], [38]. Suppose that all the receivers can achieve reliable detection, then, the outage probability of V_1 with imperfect CSI is given by

$$
OP_{V_1}^I = \underbrace{\Pr\left(\gamma_{V_1 \to x_1} < \gamma_{th1}, \gamma_{V_2 \to x_1} < \gamma_{th1}\right)}_{\Xi_1}
$$
$$
+ \underbrace{\Pr\left(\max\left(\gamma_{V_1 \to x_1}, W_1\right) < \gamma_{th1}, \gamma_{V_2 \to x_1} > \gamma_{th1}\right)}_{\Xi_2},
\tag{12}
$$

---

[1]The fixed power allocation factors and two-vehicle model are applied in this paper as most assumptions in the references. However, these concerns can be addressed in future work

[2]This scheme means that the transmitting and the receiving vehicles are located in the same lane and are in close distance to allow direct communication where possible.

[3]While either non-line-of-sight (NLOS) or line-of-sight (LOS) propagation exists in traditional V2V schemes, such a probabilistic model applied in this paper shows awareness on components of both LOS and NLOS propagation which rely on the vehicles' movement. In this scenario, a Nakagami-m fading channel model is suitable to characterize both LOS and NLOS for the V2V links [28]- [30].

where $\gamma_{thi} \triangleq 2^{R_i}-1$ and R_i is the target rate corresponding vehicle V_i, $i = 1, 2$.

Firstly, Ξ_1 is rewritten as

$$\Xi_1 = \underbrace{\Pr\left(\gamma_{V_1 \to x_1} < \gamma_{th1}\right)}_{A_1} \underbrace{\Pr\left(\gamma_{V_2 \to x_1} < \gamma_{th1}\right)}_{A_2}. \quad (13)$$

The fist term and second terms of (13) can be obtained as A_1 and A_2, respectively. in following proposition.

Proposition 1: A_1 can be computed as

$$A_1 = 1 - \sum_{i_1=0}^{m_1-1} \sum_{n_1=0}^{i_1} \binom{m_{e_1}+n_1-1}{m_{e_1}-1} \frac{\theta^{i_1} C_1^{m_{e_1}}}{(\theta+C_1)^{m_{e_1}+n_1}}$$

$$\times \frac{(H_1 \Omega_{SP}\bar\rho)^{n_1-i_1} e^{-\frac{\theta}{H_1 \Omega_{SP}\bar\rho}}}{(i_1-n_1)!} \left(1 - \frac{\Gamma\left(m_{SP}, \frac{\rho_I}{\Omega_{SP}\bar\rho}\right)}{\Gamma(m_{SP})}\right)$$

$$- \sum_{i_1=0}^{m_1-1} \sum_{n_1=0}^{i_1} \sum_{k_1=0}^{m_{SP}+n_1-1} \binom{m_{e_1}+i_1-n_1-1}{m_{e_1}-1} \binom{m_{SP}+n_1-1}{m_{SP}-1}$$

$$\times \frac{C_1^{m_{e_1}} H_1^{m_{SP}-k_1} \rho_I^{m_{SP}} (\Omega_{SP}\bar\rho)^{-k_1} \theta^{i_1} e^{-\frac{\theta+\rho_I H_1}{\bar\rho H_1 \Omega_{SP}}}}{k_1!(\theta+C_1)^{m_{e_1}+i_1-n_1}(\theta+\rho_I H_1)^{m_{SP}+n_1-k_1}} \quad (14)$$

where $\theta = \frac{\gamma_{th1}}{\alpha_1 - \gamma_{th1}\alpha_2}$, $C_i = \frac{\Omega_i}{\Omega_{e_i}}$ and $H_i = \frac{\Omega_i}{\bar\mu\Omega_{SP}}$.

Proof: See Appendix A.

Similarly, A_2 can be expressed as

$$A_2 = 1 - \sum_{i_2=0}^{m_2-1} \sum_{n_2=0}^{i_2} \binom{m_{e_2}+n_2-1}{m_{e_2}-1} \frac{\theta^{i_2} C_2^{m_{e_2}}}{(\theta+C_2)^{m_{e_2}+n_2}}$$

$$\times \frac{(H_2 \Omega_{SP}\bar\rho)^{n_2-i_2} e^{-\frac{\theta}{H_2 \Omega_{SP}\bar\rho}}}{(i_2-n_2)!} \left(1 - \frac{\Gamma\left(m_{SP}, \frac{\rho_I}{\Omega_{SP}\bar\rho}\right)}{\Gamma(m_{SP})}\right)$$

$$- \sum_{i_2=0}^{m_2-1} \sum_{n_2=0}^{i_2} \sum_{k_2=0}^{m_{SP}+n_2-1} \binom{m_{e_2}+i_2-n_2-1}{m_{e_2}-1} \binom{m_{SP}+n_2-1}{m_{SP}-1}$$

$$\times \frac{C_2^{m_{e_2}} H_2^{m_{SP}-k_2} \rho_I^{m_{SP}} (\Omega_{SP}\bar\rho)^{-k_2} \theta^{i_2} e^{-\frac{\theta+\rho_I H_2}{\bar\rho H_2 \Omega_{SP}}}}{k_2!(\theta+C_2)^{m_{e_2}+i_2-n_2}(\theta+\rho_I H_2)^{m_{SP}+n_2-k_2}}. \quad (15)$$

Substituting (14) and (15) into (13), we obtain a new equation as

$$\Xi_1 = A_1 \times A_2. \quad (16)$$

Next, the second term of (12), i.e. Ξ_2 can be expressed as

$$\Xi_2 = \Pr\left(\max\left(\gamma_{V_1 \to x_1}, W_1\right) < \gamma_{th1}, \gamma_{V_2 \to x_1} > \gamma_{th1}\right)$$

$$= \Pr\left(\gamma_{V_1 \to x_1} < \gamma_{th1}\right)$$

$$\times \Pr\left(\gamma_{V_2 \to x_1} > \gamma_{th1}\right) \Pr\left(W_1 < \gamma_{th1}\right). \quad (17)$$

First, it is denoted that $\bar{A}_i = \Pr\left(W_i < \gamma_{th1}\right)$, $C_{k,i} = \frac{\Omega_{k,i}}{\Omega_{e_{k,i}}}$ and $H_{k,i} = \frac{\Omega_{k,i}}{\bar\mu\Omega_{iP}}$. Then, with the help of (7) and (9), along

with some manipulations, $\bar{A}_i$ is formulated as.

$$\bar{A}_i = 1 - \sum_{i_{k,i}=0}^{m_{k,i}-1} \sum_{n_{k,i}=0}^{i_{k,i}} \binom{m_{e_{k,i}}+n_{k,i}-1}{m_{e_{k,i}}-1}$$

$$\frac{\gamma_{th1}^{i_1} C_{k,i}^{m_{e_{k,i}}} \left(H_{k,i}\Omega_{iP}\bar\rho\right)^{n_{k,i}-i_{k,i}} e^{-\frac{\gamma_{th1}}{H_{k,i}\Omega_{iP}\bar\rho}}}{(i_{k,i}-n_{k,i})!(\gamma_{th1}+C_{k,i})^{m_{e_{k,i}}+n_{k,i}}}$$

$$\left(1 - \frac{\Gamma\left(m_{iP}, \frac{\rho_I}{\Omega_{iP}\bar\rho}\right)}{\Gamma(m_{iP})}\right) - \sum_{i_{k,i}=0}^{m_{k,i}-1} \sum_{n_{k,i}=0}^{i_{k,i}}$$

$$\sum_{k_{k,i}=0}^{m_{iP}+n_{k,i}-1} \binom{m_{e_{k,i}}+i_{k,i}-n_{k,i}-1}{m_{e_{k,i}}-1} \binom{m_{iP}+n_{k,i}-1}{m_{iP}-1}$$

$$\frac{C_{k,i}^{m_{e_{k,i}}} H_{k,i}^{m_{iP}-k_{k,i}} \rho_I^{m_{iP}} (\Omega_{iP}\bar\rho)^{-k_{k,i}} \gamma_{th1}^{i_{k,i}} e^{-\frac{\gamma_{th1}+\rho_I H_{k,i}}{\bar\rho H_{k,i}\Omega_{iP}}}}{k_{k,i}!(\gamma_{th1}+C_{k,i})^{m_{e_{k,i}}+i_{k,i}-n_{k,i}}(\gamma_{th1}+\rho_I H_{k,i})^{m_{iP}+n_{k,i}-k_{k,i}}}. \quad (18)$$

In further computation, Ξ_2 is expressed as

$$\Xi_2 = A_1 \times (1-A_2) \times \bar{A}_1. \quad (19)$$

Finally, the outage probability in closed-form of the first vehicle can be formulated as

$$OP_{V_1}^I = \begin{cases} \Xi_1 + \Xi_2, & \gamma_{th_1} < \frac{\alpha_1}{\alpha_2} \\ 1, & \text{otherwise} \end{cases} \quad (20)$$

Depending the position of each vehicle and related interference impacts, we continue to consider outage performance of the second vehicle V_2.

B. OUTAGE PROBABILITY OF THE SECOND VEHICLE

The outage probability of V_2 is explicitly expressed in the bottom of the next page.

It is noted that Θ_1 in eq. (21) can be rewritten as

$$\Theta_1 = \Big(1 - \underbrace{\Pr\left\{\gamma_{V_2 \to x_1} > \gamma_{th1}, \gamma_{V_2 \to x_2} > \gamma_{th2}\right\}}_{B_1}\Big)$$

$$\times \Pr\left\{\gamma_{V_1 \to x_1} < \gamma_{th1}\right\}. \quad (22)$$

Proposition 2: B_1 in eq. (22) can be rewritten as

$$B_1 = \sum_{i_2=0}^{m_2-1} \sum_{n_2=0}^{i_2} \binom{m_{e_2}+n_2-1}{m_{e_2}-1} \left(\frac{\nu^{i_2} C_2^{m_{e_2}}}{(i_2-n_2)!}\right)$$

$$\times \frac{(H_2 \Omega_{SP}\bar\rho)^{n_2-i_2} e^{-\frac{\nu}{H_2 \Omega_{SP}\bar\rho}}}{(\nu+C_2)^{m_{e_2}+n_2}} \left(1 - \frac{\Gamma\left(m_{SP}, \frac{\rho_I}{\Omega_{SP}\bar\rho}\right)}{\Gamma(m_{SP})}\right)$$

$$+ \sum_{i_2=0}^{m_2-1} \sum_{n_2=0}^{i_2} \sum_{k_2=0}^{m_{SP}+n_2-1} \binom{m_{e_2}+i_2-n_2-1}{m_{e_2}-1} \binom{m_{SP}+n_2-1}{m_{SP}-1}$$

$$\times \frac{C_2^{m_{e_2}} H_2^{m_{SP}-k_2} \rho_I^{m_{SP}} (\Omega_{SP}\bar\rho)^{-k_2} \nu^{i_2} e^{-\frac{\nu+\rho_I H_2}{\bar\rho H_2 \Omega_{SP}}}}{k_2!(\nu+C_2)^{m_{e_2}+i_2-n_2}(\nu+\rho_I H_2)^{m_{SP}+n_2-k_2}}. \quad (23)$$

Proof: See Appendix B.

Eventually, Θ_1 can be formulated as

$$\Theta_1 = (1-B_1) \times A_1. \qquad (24)$$

Then, we can rewrite Θ_2 as shown.

$$
\begin{aligned}
\Theta_2 &= \Pr \left\{ \left(\gamma_{V_2 \to x_2} < \gamma_{th2} \cup \max \left(\gamma_{V_2 \to x_1}, W_2 \right) < \gamma_{th1} \right), \right. \\
&\quad \left. \gamma_{V_1 \to x_1} > \gamma_{th1} \right\} \\
&= \left[\underbrace{\Pr \left\{ \gamma_{V_2 \to x_2} < \gamma_{th2} \right\}}_{B_2} + \underbrace{\Pr \left\{ \max \left(\gamma_{V_2 \to x_1}, W_2 \right) < \gamma_{th1} \right\}}_{B_3} \right. \\
&\quad \left. - \underbrace{\Pr \left\{ \gamma_{V_2 \to x_2} < \gamma_{th2}, \gamma_{V_2 \to x_1} < \gamma_{th1}, W_2 < \gamma_{th1} \right\}}_{B_4} \right] \\
&\quad \Pr \left\{ \gamma_{V_1 \to x_1} > \gamma_{th1} \right\}
\end{aligned}
\qquad (25)
$$

First, by substituting (5) and after some required manipulations, we can obtain B_2 follows

$$B_2 = 1 - \Pr \left\{ \left| \hat{h}_2 \right|^2 > \beta_1 |e_2|^2 + \frac{\beta_1 \bar{\mu}}{\rho_S} \right\}. \qquad (26)$$

Similarly, the expression for B_2 is formulated as (27), shown at the bottom of the next page.

Next, B_3 can be rewritten as

$$
\begin{aligned}
B_3 &= \Pr \left\{ \max \left(\gamma_{V_2 \to x_1}, W_2 \right) < \gamma_{th1} \right\} \\
&= \Pr \left\{ \gamma_{V_2 \to x_1} < \gamma_{th1} \right\} \Pr \left(W_2 < \gamma_{th1} \right) \\
&= A_2 \times \bar{A}_2.
\end{aligned}
\qquad (28)
$$

In further computation, B_4 can be computed as

$$
B_4 = \underbrace{\Pr \left\{ \gamma_{V_2 \to x_2} < \gamma_{th2}, \gamma_{V_2 \to x_1} < \gamma_{th1} \right\}}_{B_{4,1}} \\
\times \Pr \left(W_2 < \gamma_{th1} \right). \qquad (29)
$$

Proposition 3: The closed-form expression of $B_{4,1}$ can be given by

$$
\begin{aligned}
B_{4,1} &= \sum_{i_2=0}^{m_2-1} \sum_{n_2=0}^{i_2} \binom{m_{e_2}+n_2-1}{m_{e_2}-1} \left(\frac{\varsigma^{i_2} C_2^{m_{e_2}}}{(i_2-n_2)!} \right) \\
&\quad \times \frac{(H_2 \Omega_{SP} \bar{\rho})^{n_2-i_2} e^{-\frac{\varsigma}{H_2 \Omega_{SP} \bar{\rho}}}}{(\varsigma+C_2)^{m_{e_2}+n_2}} \left(1 - \frac{\Gamma\left(m_{SP}, \frac{\rho_I}{\Omega_{SP}\bar{\rho}} \right)}{\Gamma(m_{SP})} \right) \\
&\quad + \sum_{i_2=0}^{m_2-1} \sum_{n_2=0}^{i_2} \sum_{k_2=0}^{m_{SP}+n_2-1} \binom{m_{e_2}+i_2-n_2-1}{m_{e_2}-1} \binom{m_{SP}+n_2-1}{m_{SP}-1}
\end{aligned}
$$

$$
\times \frac{C_2^{m_{e_2}} H_2^{m_{SP}-k_2} \rho_I^{m_{SP}} (\Omega_{SP}\bar{\rho})^{-k_2} \varsigma^{i_2} e^{-\frac{\varsigma+\rho_I H_2}{\bar{\rho} H_2 \Omega_{SP}}}}{k_2! (\varsigma+C_2)^{m_{e_2}+i_2-n_2} (\varsigma+\rho_I H_2)^{m_{SP}+n_2-k_2}}. \qquad (30)
$$

Proof: Based on (4) and (5), $B_{4,1}$ can be further rewritten as

$$
\begin{aligned}
B_{4,1} &= \Pr \left\{ \gamma_{V_2 \to x_1} < \gamma_{th1}, \gamma_{V_2 \to x_2} < \gamma_{th2} \right\} \\
&= \Pr \left\{ \frac{\left| \hat{h}_2 \right|^2 \alpha_1 \rho_S}{\left| \hat{h}_2 \right|^2 \alpha_2 \rho_S + \rho_S |e_2|^2 + \bar{\mu}} < \gamma_{th1}, \frac{\left| \hat{h}_2 \right|^2 \alpha_2 \rho_S}{\rho_S |e_2|^2 + \bar{\mu}} < \gamma_{th2} \right\} \\
&= \Pr \left\{ \left| \hat{h}_2 \right|^2 < \varsigma \left(|e_2|^2 + \frac{(\mu+1)}{\rho_S} \right) \right\},
\end{aligned}
\qquad (31)
$$

where $\varsigma = \min(\beta_1, \theta)$. Similarly, we can obtain $B_{4,1}$.

This completes the proof.

Moreover, with the help of (18), we can obtain $B_4 = B_{4,1} \times \bar{A}_2$. Then, Θ_2 is rewritten as

$$\Theta_2 = (B_2+B_3-B_4) \times A_1. \qquad (32)$$

To obtain final result, the outage probability of V_2 can be written as

$$OP_{V_2}^{pSIC} = \begin{cases} \Theta_1+\Theta_2, & \gamma_{th_1} < \frac{\alpha_1}{\alpha_2} \\ 1, & \text{otherwise} \end{cases} \qquad (33)$$

C. OUTAGE PROBABILITY OF V_2 IN CASE OF IMPERFECT SIC

In this section, it is assumed that V_2 operates in worse case of imperfect SIC (ipSIC). Therefore, the SNR of V_2 when it detects signal x_2 can be expressed as

$$\gamma_{V_2 \to x_2}^{ipSIC} = \frac{\left| \hat{h}_2 \right|^2 \alpha_2 \rho_S}{\alpha_1 \rho_S |g_2|^2 + \rho_S |e_2|^2 + \bar{\mu}}, \qquad (34)$$

where g_2 denotes the residual imperfect channel (IS). Similarly, the outage probability of V_2 is given by

$$OP_{V_2}^{ipSIC} = \bar{\Theta}_1 + \bar{\Theta}_2, \qquad (35)$$

where $\bar{\Theta}_1 = \left(1-\bar{B}_1\right) A_1$ and $\Theta_2 = \left(\bar{B}_2+B_3-\bar{B}_4 \bar{A}_2\right)(1-A_1)$.

Proposition 4: $\bar{B}_1$ can be calculated as follows

$$\bar{B}_1 = \begin{cases} J_1+J_2+J_3+J_4 & \text{if}: \theta > \beta_1 \\ J_5+J_6 & \text{if}: \theta \leqslant \beta_1 \end{cases} \qquad (36)$$

where J_1, J_2, J_3, J_4, J_5 and J_6 are shown in the appendix C.

Proof: See Appendix C.

$$
OP_{V_2}^{pSIC} = \underbrace{\Pr \left\{ \left(\gamma_{V_2 \to x_2} < \gamma_{th2} \cup \gamma_{V_2 \to x_1} < \gamma_{th1} \right), \gamma_{V_1 \to x_1} < \gamma_{th1} \right\}}_{\Theta_1}
$$

$$
+ \underbrace{\Pr \left\{ \left(\gamma_{V_2 \to x_2} < \gamma_{th2} \cup \max \left(\gamma_{V_2 \to x_1}, W_2 \right) < \gamma_{th1} \right), \gamma_{V_1 \to x_1} > \gamma_{th1} \right\}}_{\Theta_2}. \qquad (21)
$$

Proposition 5: $\bar{B}_2$ can be expressed as

$$
\begin{aligned}
\bar{B}_2 &= 1 - \sum_{i_2=0}^{m_2-1} \sum_{p_2=0}^{i_2} \sum_{n_2=0}^{p_2} \binom{m_{e_2}+n_2-1}{m_{e_2}-1} \binom{m_2+i_2-p_2-1}{m_2-1} \\
&\quad \times \frac{C_2^{m_{e_2}} \bar{\xi}^{i_2-p_2} \beta_1^{p_2} e^{-\frac{\beta_1}{H_2 \Omega_{SP}\bar{\rho}}} \left(1-\frac{\Gamma(m_{SP}, \rho_I/(\bar{\rho}\Omega_{SP}))}{\Gamma(m_{SP})}\right)}{(p_2-n_2)!(H_2 \Omega_{SP}\bar{\rho})^{p_2-n_2}(\bar{\xi}+1)^{m_2+i_2-p_2}(\beta_1+C_2)^{m_{e_2}+n_2}} \\
&\quad - \sum_{i_2=0}^{m_2-1} \sum_{p_2=0}^{i_2} \sum_{n_2=0}^{p_2} \binom{m_{e_2}+p_2-n_2-1}{m_{e_2}-1} \binom{m_2+i_2-p_2-1}{m_2-1} \\
&\quad \times \frac{C_2^{m_{e_2}}(\beta_1+C_2)^{-m_{e_2}-p_2+n_2} \bar{\xi}^{i_2-p_2}\beta_1^{p_2}(H_2\rho_I)^{m_{SP}}}{n_2! \Gamma(m_{SP}) (\bar{\xi}+1)^{m_2+i_2-p_2}(\beta_1+H_2\rho_I)^{m_{SP}+n_2}} \\
&\quad \times \Gamma\left(m_{SP}+n_2, \frac{\beta_1+H_2\rho_I}{H_2 \Omega_{SP}\bar{\rho}}\right).
\end{aligned}
\tag{37}
$$

Proof: $\bar{B}_2$ can be written as

$$
\begin{aligned}
\bar{B}_2 &= 1 - \Pr\left\{|\hat{h}_2|^2 > \gamma_{th2}\bar{\alpha}|g_2|^2 + \beta_1\left(|e_2|^2 + \frac{\bar{\mu}}{\bar{\rho}}\right),\right. \\
&\quad \left. |h_{SP}|^2 < \frac{\rho_I}{\bar{\rho}}\right\} - \Pr\left\{|\hat{h}_2|^2 > \gamma_{th2}\bar{\alpha}|g_2|^2 \right. \\
&\quad \left. + \beta_1\left(|e_2|^2 + \frac{\bar{\mu}|h_{SP}|^2}{\rho_I}\right), |h_{SP}|^2 > \frac{\rho_I}{\bar{\rho}}\right\}.
\end{aligned}
\tag{38}
$$

Then, it can be further shown that

$$
\begin{aligned}
\bar{B}_2 &= 1 - F_{|h_{SP}|^2}\left(\frac{\rho_I}{\bar{\rho}}\right) \int_0^\infty f_{|g_2|^2}(z) \int_0^\infty f_{|e_2|^2}(y) \\
&\quad \times \bar{F}_{|\hat{h}_2|^2}\left(\gamma_{th2}\bar{\alpha}z + \beta_1\left(y+\frac{\bar{\mu}}{\bar{\rho}}\right)\right) dy dz \\
&\quad - \int_{\frac{\rho_I}{\bar{\rho}}}^\infty f_{|h_{SP}|^2}(t) \int_0^\infty f_{|g_2|^2}(z) \int_0^\infty f_{|e_2|^2}(y) \\
&\quad \times \bar{F}_{|\hat{h}_2|^2}\left(\gamma_{th2}\bar{\alpha}z + \beta_1\left(y+\frac{\bar{\mu}t}{\rho_I}\right)\right) dy dz dt.
\end{aligned}
\tag{39}
$$

Similarly, after some substitutions and manipulations we can obtain (39).

It completes the proof.

Next, B_4 can be expressed as

$$
\begin{aligned}
\bar{B}_4 &= 1 - \Pr\left\{\gamma_{V_2 \to x_2} > \gamma_{th2} \cup \gamma_{V_2 \to x_1} > \gamma_{th1}\right\} \\
&= 1 - \left(\Pr\left\{\gamma_{V_2 \to x_2} > \gamma_{th2}\right\} + \Pr\left\{\gamma_{V_2 \to x_1} > \gamma_{th1}\right\}\right.
\end{aligned}
$$

$$
\begin{aligned}
&\quad \left. - \Pr\left\{\gamma_{V_2 \to x_2} > \gamma_{th2} \cup \gamma_{V_2 \to x_1} > \gamma_{th1}\right\}\right) \\
&= \bar{B}_2 + A_2 + \bar{B}_1 - 1.
\end{aligned}
\tag{40}
$$

Finally, with the help of (36), (37) and (40), we can obtain the closed-form expression of V_2.

IV. SCHEME II: NOMA-V2X WITHOUT V2V LINK

This scheme does not allow V2V link. Due to similar way in computation, we present expression of the outage probability for the vehicle V_1 as

$$
OP_{V_1}^{II} = 1 - \Pr\left(\gamma_{V_1 \to x_1} > \gamma_{th1}\right).
\tag{41}
$$

Similarly, with the help of Proposition 1, the closed-form expression of outage probability of the vehicle V_1 in Scheme II can be expressed as

$$
\begin{aligned}
OP_{V_1}^{II} &= 1 - \sum_{i_1=0}^{m_1-1} \sum_{n_1=0}^{i_1} \binom{m_{e_1}+n_1-1}{m_{e_1}-1} \frac{\theta^{i_1} C_1^{m_{e_1}}}{(\theta+C_1)^{m_{e_1}+n_1}} \\
&\quad \times \frac{(H_1 \Omega_{SP}\bar{\rho})^{n_1-i_1} e^{-\frac{\theta}{H_1 \Omega_{SP}\bar{\rho}}}}{(i_1-n_1)!} \left(1-\frac{\Gamma\left(m_{SP}, \frac{\rho_I}{\Omega_{SP}\bar{\rho}}\right)}{\Gamma(m_{SP})}\right) \\
&\quad - \sum_{i_1=0}^{m_1-1} \sum_{n_1=0}^{i_1} \sum_{k_1=0}^{m_{SP}+n_1-1} \binom{m_{e_1}+i_1-n_1-1}{m_{e_1}-1} \binom{m_{SP}+n_1-1}{m_{SP}-1} \\
&\quad \times \frac{C_1^{m_{e_1}} H_1^{m_{SP}-k_1} \rho_I^{m_{SP}} (\Omega_{SP}\bar{\rho})^{-k_1} \theta^{i_1} e^{-\frac{\theta+\rho_I H_1}{\bar{\rho}H_1 \Omega_{SP}}}}{k_1!(\theta+C_1)^{m_{e_1}+i_1-n_1}(\theta+\rho_I H_1)^{m_{SP}+n_1-k_1}}.
\end{aligned}
\tag{42}
$$

Next, we consider the outage probability of the vehicle V_2 in a perfect SIC scenario and it is given by

$$
OP_{V_2}^{II,pSIC} = 1 - \Pr\left\{\gamma_{V_2 \to x_1} > \gamma_{th1}, \gamma_{V_2 \to x_2} > \gamma_{th2}\right\}.
\tag{43}
$$

Similarly, the closed-form expression of outage probability for the vehicle V_2 is formulated by

$$
\begin{aligned}
OP_{V_2}^{II,pSIC} &= 1 - \sum_{i_2=0}^{m_2-1} \sum_{n_2=0}^{i_2} \binom{m_{e_2}+n_2-1}{m_{e_2}-1} \left(\frac{v^{i_2} C_2^{m_{e_2}}}{(i_2-n_2)!}\right) \\
&\quad \times \frac{(H_2 \Omega_{SP}\bar{\rho})^{n_2-i_2} e^{-\frac{v}{H_2 \Omega_{SP}\bar{\rho}}}}{(v+C_2)^{m_{e_2}+n_2}} \left(1-\frac{\Gamma\left(m_{SP}, \frac{\rho_I}{\Omega_{SP}\bar{\rho}}\right)}{\Gamma(m_{SP})}\right) \\
&\quad + \sum_{i_2=0}^{m_2-1} \sum_{n_2=0}^{i_2} \sum_{k_2=0}^{m_{SP}+n_2-1} \binom{m_{e_2}+i_2-n_2-1}{m_{e_2}-1} \binom{m_{SP}+n_2-1}{m_{SP}-1}
\end{aligned}
$$

$$
\begin{aligned}
B_2 &= 1 - \sum_{i_2=0}^{m_2-1} \sum_{n_2=0}^{i_2} \binom{m_{e_2}+n_2-1}{m_{e_2}-1} \frac{\beta_1^{i_2} C_2^{m_{e_2}}(H_2 \Omega_{SP}\bar{\rho})^{n_2-i_2} e^{-\frac{\beta_1}{H_2 \Omega_{SP}\bar{\rho}}}}{(i_2-n_2)!(\beta_1+C_2)^{m_{e_2}+n_2}} \left(1-\frac{\Gamma\left(m_{SP}, \frac{\rho_I}{\Omega_{SP}\bar{\rho}}\right)}{\Gamma(m_{SP})}\right) \\
&\quad - \sum_{i_2=0}^{m_2-1} \sum_{n_2=0}^{i_2} \sum_{k_2=0}^{m_{SP}+n_2-1} \binom{m_{e_2}+i_2-n_2-1}{m_{e_2}-1} \binom{m_{SP}+n_2-1}{m_{SP}-1} \frac{C_2^{m_{e_2}} H_2^{m_{SP}-k_2} \rho_I^{m_{SP}} (\Omega_{SP}\bar{\rho})^{-k_2} \beta_1^{i_2} e^{-\frac{\beta_1+\rho_I H_2}{\bar{\rho}H_2 \Omega_{SP}}}}{k_2!(\beta_1+C_2)^{m_{e_2}+i_2-n_2}(\beta_1+\rho_I H_2)^{m_{SP}+n_2-k_2}}
\end{aligned}
\tag{27}
$$

$$\times \frac{C_2^{m_{e_2}} H_2^{m_{SP}-k_2} \rho_I^{m_{SP}} (\Omega_{SP}\bar{\rho})^{-k_2} v^{i_2} e^{-\frac{v+\rho_I H_2}{\bar{\rho} H_2 \Omega_{SP}}}}{k_2! (v+C_2)^{m_{e_2}+i_2-n_2} (v+\rho_I H_2)^{m_{SP}+n_2-k_2}}. \tag{44}$$

In case of imperfect SIC, the outage probability of the vehicle V_2 is expressed as

$$OP_{V_2}^{II,ipSIC} = 1-\Pr\left\{\gamma_{V_2 \to x_1} > \gamma_{th1}, \gamma_{V_2 \to x_2}^{ipSIC} > \gamma_{th2}\right\}. \tag{45}$$

Similar to the derivation reported in Scheme I, the closed-form expression of outage performance for the vehicle V_1 is given as

$$OP_{V_2}^{II,pSIC} = \begin{cases} 1-J_1-J_2-J_3-J_4 & if : \theta > \beta_1 \\ 1-J_5-J_6 & if : \theta \le \beta_1 \end{cases} \tag{46}$$

V. APPROXIMATION ANALYSIS OF OUTAGE PROBABILITY AND THROUGHPUT

There are more insights to show performance of the considered system. First, the throughput can be achieved from outage probability. Then, asymptotic outage performance is careful computed.

A. THROUGHPUT PERFORMANCE ANALYSIS

It is necessary to examine other metric to further provide evaluation for each destination and the overall throughput to characterize system performance with $z \in \{pSIC, ipSIC\}$. Such throughput depends on the probability outage which occurs following fixed target rates R_1 and R_2. Furthermore, optimal performance of throughput can be captured by performing method of the numerical simulations. In particular, the throughput of system can be given as

$$T^z = R_1\left(1-OP_{V_1}\right)+R_2\left(1-OP_{V_2}^z\right). \tag{47}$$

Since deriving closed-form expressions are intractable, computation of the asymptotic expressions are necessary to explicit evaluate the outage performance.

B. ASYMPTOTIC EXPRESSIONS WITH $\bar{\rho}_S \to \infty$

In this section, when $\bar{\rho}_S \to \infty$ we consider the following probability

$$A_1^{\bar{\rho}_S \to \infty} = 1-\Pr\left(\frac{\left|\hat{h}_1\right|^2 \alpha_1 \rho_I}{\left|\hat{h}_1\right|^2 \alpha_2 \rho_I + |e_1|^2 \rho_I + |h_{SP}|^2 \bar{\mu}} > \gamma_{th1}\right). \tag{48}$$

Then, based on the PDF and CDF of the related channels, we can obtain $A_1^{\bar{\rho}_S \to \infty}$ as

$$A_1^{\bar{\rho}_S \to \infty} = 1-\sum_{i_1=0}^{m_1-1}\sum_{k_1=0}^{i_1}\binom{m_{SP}+k_1-1}{m_{SP}-1}\frac{(H_1\rho_I)^{m_{SP}}}{(H_1\rho_I+\theta)^{m_{SP}+k_1}}$$
$$\times \binom{m_{e_1}+i_1-k_1-1}{m_{e_1}-1}\frac{\theta^{i_1}C_1^{m_{e_1}}}{(C_1+\theta)^{m_{e_1}+i_1-k_1}}. \tag{49}$$

Similarly, $A_2^{\bar{\rho}_S \to \infty}$ and $\bar{A}_i^{\bar{\rho}_S \to \infty}$ are obtained respectively as

$$A_2^{\bar{\rho}_S \to \infty} = 1-\sum_{i_2=0}^{m_2-1}\sum_{k_2=0}^{i_2}\binom{m_{SP}+k_2-1}{m_{SP}-1}\frac{(H_2\rho_I)^{m_{SP}}}{(H_2\rho_I+\theta)^{m_{SP}+k_2}}$$
$$\times \binom{m_{e_2}+i_2-k_2-1}{m_{e_2}-1}\frac{\theta^{i_2}C_2^{m_{e_2}}}{(C_2+\theta)^{m_{e_2}+i_2-k_2}}. \tag{50}$$

and

$$\bar{A}_i^{\bar{\rho}_S \to \infty}$$
$$= 1-\sum_{i_{k,i}=0}^{m_{k,i}-1}\sum_{k_{k,i}=0}^{i_{k,i}}\binom{m_{SP}+k_{k,i}-1}{m_{SP}-1}\left(H_{k,i}\rho_I\right)^{m_{SP}}\gamma_{th1}^{i_{k,i}}$$
$$\times \binom{m_{e_{k,i}}+i_{k,i}-k_{k,i}-1}{m_{e_{k,i}}-1}\frac{C_{k,i}^{m_{e_{k,i}}}\left(H_{k,i}\rho_I+\gamma_{th1}\right)^{-m_{SP}-k_{k,i}}}{(C_1+\gamma_{th1})^{m_{e_{k,i}}+i_{k,i}-k_{k,i}}}. \tag{51}$$

Therefore, the asymptotic of the first vehicle V_1 in Scheme I is given by

$$OP_{V_1}^{I,\bar{\rho}_S \to \infty} = \Xi_1^{\bar{\rho}_S \to \infty}+\Xi_2^{\bar{\rho}_S \to \infty}, \tag{52}$$

where $\Xi_1^{\bar{\rho}_S \to \infty} = A_1^{\bar{\rho}_S \to \infty} \times A_2^{\bar{\rho}_S \to \infty}$ and $\Xi_2^{\bar{\rho}_S \to \infty} = A_1^{\bar{\rho}_S \to \infty} \times (1-A_2^{\bar{\rho}_S \to \infty}) \times \bar{A}_1^{\bar{\rho}_S \to \infty}$.

In next step, it can be achieved $B_1^{\bar{\rho}_S \to \infty}$ as

$$B_1^{\bar{\rho}_S \to \infty} = 1-\sum_{i_2=0}^{m_2-1}\sum_{k_2=0}^{i_2}\binom{m_{SP}+k_2-1}{m_{SP}-1}\frac{(H_2\rho_I)^{m_{SP}}}{(H_2\rho_I+v)^{m_{SP}+k_2}}$$
$$\times \binom{m_{e_2}+i_2-k_2-1}{m_{e_2}-1}\frac{v^{i_2}C_2^{m_{e_2}}}{(C_2+v)^{m_{e_2}+i_2-k_2}}. \tag{53}$$

Moreover, $B_2^{\bar{\rho}_S \to \infty}$ and $B_{4,1}^{\rho_S \to \infty}$ are formulated respectively in similar way as

$$B_2^{\bar{\rho}_S \to \infty} = 1-\sum_{i_2=0}^{m_2-1}\sum_{k_2=0}^{i_2}\binom{m_{SP}+k_2-1}{m_{SP}-1}\frac{(H_2\rho_I)^{m_{SP}}}{(H_2\rho_I+\beta_1)^{m_{SP}+k_2}}$$
$$\times \binom{m_{e_2}+i_2-k_2-1}{m_{e_2}-1}\frac{\beta_1^{i_2}C_2^{m_{e_2}}}{(C_2+\beta_1)^{m_{e_2}+i_2-k_2}}, \tag{54}$$

and

$$B_{4,1}^{\bar{\rho}_S \to \infty} = 1-\sum_{i_2=0}^{m_2-1}\sum_{k_2=0}^{i_2}\binom{m_{SP}+k_2-1}{m_{SP}-1}\frac{(H_2\rho_I)^{m_{SP}}}{(H_2\rho_I+\varsigma)^{m_{SP}+k_2}}$$
$$\times \binom{m_{e_2}+i_2-k_2-1}{m_{e_2}-1}\frac{\varsigma^{i_2}C_2^{m_{e_2}}}{(C_2+\varsigma)^{m_{e_2}+i_2-k_2}}. \tag{55}$$

Thus, the asymptotic of the second vehicle V_2 in Scheme I is obtained as

$$OP_{V_2}^{I,pSIC,\bar{\rho}_S \to \infty} = \Theta_1^{\bar{\rho}_S \to \infty}+\Theta_2^{\bar{\rho}_S \to \infty}, \tag{56}$$

where $\Theta_1^{\bar{\rho}_S \to \infty} = (1-B_1^{\bar{\rho}_S \to \infty}) \times A_1^{\bar{\rho}_S \to \infty}$, $B_3^{\bar{\rho}_S \to \infty} = A_2^{\bar{\rho}_S \to \infty} \times \bar{A}_2^{\bar{\rho}_S \to \infty}$, $B_4^{\bar{\rho}_S \to \infty} = B_{4,1}^{\rho_S \to \infty} \times \bar{A}_2^{\bar{\rho}_S \to \infty}$ and $\Theta_2^{\bar{\rho}_S \to \infty} = (B_2^{\bar{\rho}_S \to \infty}+B_3^{\bar{\rho}_S \to \infty}-B_4^{\bar{\rho}_S \to \infty}) \times (1-A_1^{\rho_S \to \infty})$.

In case of ipSIC, we can express the asymptotic of V_2 as

$$OP_{V_2}^{I,ipSIC,\bar{\rho}_S \to \infty} = \bar{\Theta}_1^{\bar{\rho}_S \to \infty} + \bar{\Theta}_2^{\bar{\rho}_S \to \infty}, \qquad (57)$$

where $\bar{\Theta}_1^{\bar{\rho}_S \to \infty} = \left(1 - \bar{B}_1^{\bar{\rho}_S \to \infty}\right) A_1^{\bar{\rho}_S \to \infty}$ and $\bar{\Theta}_2^{\bar{\rho}_S \to \infty} = \left(\bar{B}_2^{\bar{\rho}_S \to \infty} + B_3^{\bar{\rho}_S \to \infty} - \bar{B}_4^{\bar{\rho}_S \to \infty} \bar{A}_2^{\bar{\rho}_S \to \infty}\right) (1 - A_1^{\bar{\rho}_S \to \infty})$.

Proposition 6: $\bar{B}_1^{\bar{\rho}_S \to \infty}$ can be obtained as

$$\bar{B}_1^{\bar{\rho}_S \to \infty} = \begin{cases} K_1 + K_2 & \text{if} : \theta > \beta_1 \\ \bar{K} & \text{if} : \theta \leqslant \beta_1 \end{cases} \qquad (58)$$

Proof: See in Appendix D.

In similar way, $B_2^{\bar{\rho}_S \to \infty}$ can be expressed as

$$\bar{B}_2^{\bar{\rho}_S \to \infty} = \sum_{i_2=0}^{m_2-1} \sum_{p_2=0}^{i_2} \sum_{n_2=0}^{p_2} \binom{m_{e_2}+p_2-n_2-1}{m_{e_2}-1}$$
$$\times \binom{m_2+i_2-p_2-1}{m_2-1} \binom{m_{SP}+n_2-1}{m_{SP}-1}$$
$$\times \frac{\beta_1^{p_2} \bar{\xi}^{i_2-p_2} C_2^{m_{e_2}} (\rho_I H_2)^{m_{SP}} (\bar{\xi}+1)^{p_2-m_2-i_2}}{(\beta_1+C_2)^{m_{e_2}+p_2-n_2} (\beta_1+H_2\rho_I)^{m_{SP}+n_2}}. \qquad (59)$$

Finally, the asymptotic outage probability of the second vehicle V_2 in case ipSIC is written as

$$OP_{V_2}^{I,ipSIC,\bar{\rho}_S \to \infty} = \bar{\Theta}_1^{\bar{\rho}_S \to \infty} + \bar{\Theta}_2^{\bar{\rho}_S \to \infty}, \qquad (60)$$

where $\bar{\Theta}_1^{\bar{\rho}_S \to \infty} = \left(1 - \bar{B}_1^{\bar{\rho}_S \to \infty}\right) A_1^{\bar{\rho}_S \to \infty}$ and $\bar{\Theta}_2^{\bar{\rho}_S \to \infty} = \left(\bar{B}_2^{\bar{\rho}_S \to \infty} + B_3^{\bar{\rho}_S \to \infty} - \bar{B}_4^{\bar{\rho}_S \to \infty} \bar{A}_2^{\bar{\rho}_S \to \infty}\right) (1 - A_1^{\bar{\rho}_S \to \infty})$.

By performing similar steps in Scheme I, we can express the asymptotic outage probabilities in Scheme II, i.e. for V_1 as $OP_{V_1}^{II,\bar{\rho}_S \to \infty} = A_1^{\bar{\rho}_S \to \infty}$, for the asymptotic of V_2 in case pSIC as $OP_{V_2}^{II,pSIC,\bar{\rho}_S \to \infty} = 1 - B_1^{\bar{\rho}_S \to \infty}$ and for the asymptotic of V_2 in case of ipSIC as $OP_{V_2}^{II,ipSIC,\bar{\rho}_S \to \infty} = 1 - \bar{B}_1^{\bar{\rho}_S \to \infty}$.

C. ASYMPTOTIC EXPRESSIONS WITH $\rho_I \to \infty$

When $\rho_I \to \infty$ we can write A_i as

$$A_i^{\rho_I \to \infty} = 1 - \Pr\left(\frac{\left|\hat{h}_i\right|^2 \alpha_1 \bar{\rho}_S}{\left|\hat{h}_i\right|^2 \alpha_2 \bar{\rho}_S + |e_i|^2 \bar{\rho}_S + \bar{\mu}} > \gamma_{th1}\right)$$
$$= 1 - \sum_{i_i=0}^{m_i-1} \sum_{n_i=0}^{i_i} \binom{m_{e_i}+n_1-1}{m_{e_i}-1}$$
$$\times \frac{\theta^{i_i} C_i^{m_{e_i}} (H_1\Omega_{SP}\bar{\rho})^{n_i-i_i} e^{-\frac{\theta}{H_i\Omega_{SP}\bar{\rho}}}}{(i_i-n_i)! (\theta+C_i)^{m_{e_i}+n_i}}. \qquad (61)$$

Similarly, we can rewrite $\bar{A}_i^{\rho_I \to \infty}$ as

$$\bar{A}_i = 1 - \sum_{i_{k,i}=0}^{m_{k,i}-1} \sum_{n_{k,i}=0}^{i_{k,i}} \binom{m_{e_{k,i}}+n_{k,i}-1}{m_{e_{k,i}}-1}$$
$$\times \frac{\gamma_{th1}^{i_1} C_{k,i}^{m_{e_{k,i}}} (H_{k,i}\Omega_{iP}\bar{\rho})^{n_{k,i}-i_{k,i}} e^{-\frac{\gamma_{th1}}{H_{k,i}\Omega_{iP}\bar{\rho}}}}{(i_{k,i}-n_{k,i})! (\gamma_{th1}+C_{k,i})^{m_{e_{k,i}}+n_{k,i}}}. \qquad (62)$$

Thus, relying on (61) and (62), we have the asymptotic outage probability of V_1 as

$$OP_{V_1}^{I,\rho_I \to \infty} = \Xi_1^{\rho_I \to \infty} + \Xi_2^{\rho_I \to \infty}, \qquad (63)$$

where $\Xi_1^{\rho_I \to \infty} = A_1^{\rho_I \to \infty} \times A_2^{\rho_I \to \infty}$ and $\Xi_2^{\rho_I \to \infty} = A_1^{\rho_I \to \infty} \times (1 - A_2^{\rho_I \to \infty}) \times \bar{A}_1^{\rho_I \to \infty}$.

Then, to achieve $OP_{V_2}^{I,pSIC}$, we need compute $B_1^{\rho_I \to \infty}$ and $B_2^{\rho_I \to \infty}$ as

$$B_1^{\rho_I \to \infty} = \sum_{i_2=0}^{m_2-1} \sum_{n_2=0}^{i_2} \binom{m_{e_2}+n_2-1}{m_{e_2}-1}$$
$$\times \frac{v^{i_2} C_2^{m_{e_2}} (H_2\Omega_{SP}\bar{\rho})^{n_2-i_2} e^{-\frac{v}{H_2\Omega_{SP}\bar{\rho}}}}{(i_2-n_2)! (v+C_2)^{m_{e_2}+n_2}}. \qquad (64)$$

and

$$B_2^{\rho_I \to \infty} = 1 - \sum_{i_2=0}^{m_2-1} \sum_{n_2=0}^{i_2} \binom{m_{e_2}+n_2-1}{m_{e_2}-1}$$
$$\times \frac{\beta_1^{i_2} C_2^{m_{e_2}} (H_2\Omega_{SP}\bar{\rho})^{n_2-i_2} e^{-\frac{\beta_1}{H_2\Omega_{SP}\bar{\rho}}}}{(i_2-n_2)! (\beta_1+C_2)^{m_{e_2}+n_2}}. \qquad (65)$$

Moreover, the asymptotic outage probability of V_2 in case of pSIC is computed by

$$OP_{V_2}^{I,pSIC} = \Theta_1^{\rho_I \to \infty} + \Theta_2^{\rho_I \to \infty}, \qquad (66)$$

where $\Theta_1^{\rho_I \to \infty} = \left(1 - B_1^{\rho_I \to \infty}\right) \times A_1^{\rho_I \to \infty}$, $\Theta_2^{\rho_I \to \infty} = (B_2^{\rho_I \to \infty} + B_3^{\rho_I \to \infty} - B_4^{\rho_I \to \infty}) \times (1 - A_1^{\rho_I \to \infty})$, $B_4^{\rho_I \to \infty} = B_{4,1}^{\rho_I \to \infty} \times \bar{A}_2^{\rho_I \to \infty}$ and $B_{4,1}^{\rho_I \to \infty}$ can be obtained similarly as (64).

Next, in case of ipSIC we can obtain the asymptotic outage probability of V_2 as

$$OP_{V_2}^{I,ipSIC,\rho_I \to \infty} = \bar{\Theta}_1^{\rho_I \to \infty} + \bar{\Theta}_2^{\rho_I \to \infty}, \qquad (67)$$

where $\bar{\Theta}_1^{\rho_I \to \infty} = \left(1 - \bar{B}_1^{\rho_I \to \infty}\right) A_1^{\rho_I \to \infty}$ and $\bar{\Theta}_2^{\rho_I \to \infty} = \left(\bar{B}_2^{\rho_I \to \infty} + B_3^{\rho_I \to \infty} - \bar{B}_4^{\rho_I \to \infty} \bar{A}_2^{\rho_I \to \infty}\right) (1 - A_1^{\rho_I \to \infty})$. Similarly, $\bar{B}_2^{\rho_I \to \infty}$ is easy obtain it.

It is worth noting that the following outage probability can be computed in similar way

$$\bar{B}_1^{\rho_I \to \infty} = \Pr\left\{\left|\hat{h}_2\right|^2 > \gamma_{th2}\bar{\alpha} |g_2|^2 + \beta_1 \left(|e_2|^2 + \frac{\bar{\mu}}{\bar{\rho}}\right),\right.$$
$$\left.\left|\hat{h}_2\right|^2 > \theta \left(|e_2|^2 + \frac{\bar{\mu}}{\bar{\rho}}\right)\right\}. \qquad (68)$$

It can be obtained $\bar{B}_1^{\rho_I \to \infty}$ as

$$\bar{B}_1^{\rho_I \to \infty} = \begin{cases} M_1 + M_2 & \text{if} : \theta > \beta_1 \\ \bar{M} & \text{if} : \theta \leqslant \beta_1 \end{cases} \qquad (69)$$

It is noted that if $\theta > \beta_1$ M_1 is given by

$$M_1 = \sum_{i_2=0}^{m_2-1} \sum_{p_2=0}^{i_2} \binom{m_{e_2}+i_2-p_2-1}{m_{e_2}-1}$$

$$\times \frac{C_2^{m_{e_2}} \theta^{i_2} (\theta + C_2)^{-m_{e_2} - i_2 + p_2} e^{-\frac{\theta}{H_2 \Omega_{SP} \bar{\rho}}}}{p_2! (H_2 \Omega_{SP} \bar{\rho})^{p_2}}$$

$$- \sum_{i_2=0}^{m_2-1} \sum_{p_2=0}^{m_2-1} \sum_{n_2=0}^{i_2+p_2} \binom{m_{e_2} + i_2 + p_2 - n_2 - 1}{m_{e_2} - 1} \binom{i_2 + p_2}{i_2}$$

$$\times \frac{C_2^{m_{e_2}} \theta^{p_2} (\theta - \beta_1)^{i_2} \bar{\zeta}^{m_{e_2} + p_2 - n_2} e^{-\frac{\psi}{\zeta H_2 \Omega_{SP} \bar{\rho}}}}{n_2! (H_2 \Omega_{SP} \bar{\rho})^{n_2} (\psi + \bar{\zeta} C_2)^{m_{e_2} + i_2 + p_2 - n_2}}, \quad (70)$$

and

$$M_2 = \sum_{i_2=0}^{m_2-1} \sum_{p_2=0}^{i_2} \sum_{n_2=0}^{m_2+i_2-p_2-1} \sum_{k_2=0}^{p_2+n_2} \binom{m_2 + i_2 - p_2 - 1}{m_2 - 1}$$

$$\times \binom{m_{e_2} + k_2 - 1}{m_{e_2} - 1} \binom{p_2 + n_2}{p_2} \frac{\beta_1^{p_2} C_2^{m_{e_2}} (\psi - \beta_1 \bar{\zeta})^{n_2}}{(p_2 + n_2 - k_2)!}$$

$$\times \frac{(\bar{\zeta} + 1)^{-m_2 - i_2 + p_2} e^{-\frac{\psi}{\zeta H_2 \Omega_{SP} \bar{\rho}}}}{(\bar{\zeta} H_2 \Omega_{SP} \bar{\rho})^{p_2 + n_2 - k_2} (\psi + \bar{\zeta} C_2)^{m_{e_2} + k_2} \bar{\zeta}^{-m_{e_2} - i_2}}. \quad (71)$$

In case $\theta < \beta_1$ we have

$$\bar{M} = \sum_{i_2=0}^{m_2-1} \sum_{p_2=0}^{i_2} \sum_{n_2=0}^{p_2} \binom{m_2 + i_2 - p_2 - 1}{m_2 - 1}$$

$$\times \binom{m_{e_2} + p_2 - n_2 - 1}{m_{e_2} - 1} \frac{\beta_1^{p_2} C_2^{m_{e_2}} e^{-\frac{\beta_1}{H_2 \Omega_{SP} \bar{\rho}}}}{(\beta_1 + C_2)^{m_{e_2} + p_2 - n_2}}$$

$$\times \frac{\bar{\zeta}^{i_2 - p_2}}{n_2! (\bar{\zeta} + 1)^{m_2 + i_2 - p_2} (H_2 \Omega_{SP} \bar{\rho})^{n_2}}. \quad (72)$$

Similarly, in Scheme II when $\rho_I \to \infty$ we also have similar expressions. We omit here due to its simplicity.

VI. SIMULATION RESULT AND DISCUSSION

The simulation model is based on Fig. 1, and we assume fixed power allocation factors assigned for the two NOMA vehicles such that $\alpha_1 = 0.8$ and $\alpha_2 = 0.2$. In the simulations, we set $\lambda_{SP} = \lambda_{iP} = \lambda_{k,i} = 0.1$, $\lambda_1 = 0.5$, $\lambda_2 = 1$, $\lambda_e = \lambda_{eSR} = \lambda_{e_i} = \lambda_{e_{k,i}}$, $\mu = 0.5$, $m = m_{SR} = m_1 = m_2 = m_{SP} = m_{1P} = m_{2P} = m_{k,i}$ and $R = R_1 = R_2$ (BPCU) except for specific cases, in which BPCU is short for bit per channel use.

Figs. 2 and 3 show the outage performance for the two schemes versus the transmit SNR at the BS $\bar{\rho}_S$ and ρ_I respectively to illustrate the performance gap among two vehicles in the CR-assisted NOMA-V2X scenario with target rates $R = 1(BPCU)$ (it is assumed that $R_1 = R_2 = R$ from now onward). It is clear that performance gap among two schemes for each vehicle becomes larger at SNR high region. The outage performance of the vehicle V_2 is better than V_1. This observation is explained by different SIC and signal detection conditions. It can be further confirmed that the outage performance meet saturation at high SNR for Fig. 2 and Fig. 3. It can be explained that such result is obtained straightforward from definition of outage probability. Precisely, asymptotic lines of outage probabilities meet exact curves at high region of $\bar{\rho}_S$
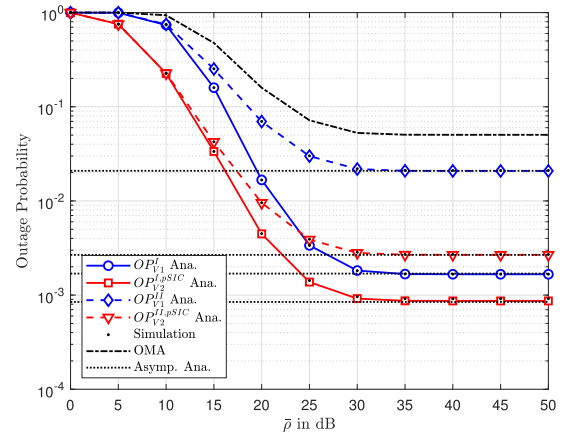

FIGURE 2. Outage performance of V_1 and V_2 versus $\bar{\rho}$ with $\lambda_e = \zeta = 0.01$, $m = 2$, $\rho_I = 20$dB and $R = 1$ (BPCU).

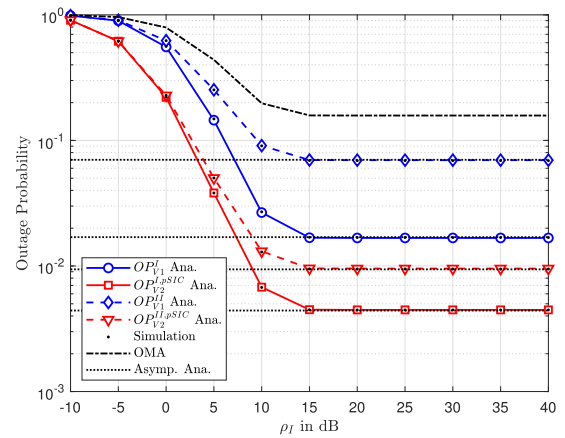**FIGURE 3.** Outage performance of V_1 and V_2 versus ρ_I with $\lambda_e = \zeta = 0.01$, $m = 2$, $\bar{\rho} = 20$ dB and $R = 1$ (BPCU).

and ρ_I. These figures indicates that the well matching exists between analytical result and Monte-Carlo simulation result. Such matching observations are also illustrated in following experiments. Then, the correctness of analytical results is verified.

Fig. 4 shows different levels of CSI imperfections to such system for the two schemes under consideration. Such CSI term has impacts on the outage probability of V_1 and V_2. When increasing the CSI level λ_e, outage performance of the two vehicles become worse. It is noted that due to λ_e affecting the achievable SINR, $\lambda_e = 0.1$ leads to small performance gap among two vehicles. Therefore, by limiting CSI imperfections it is possible to maintain outage performance at reasonable value. In Fig. 4, it is easily noticeable that outage performance of vehicle V_2 is still better than that of V_1.

To look at impact of fading parameter m on the outage performance of the two schemes, we plot outage performance versus the transmit SNR $\bar{\rho}$ in Fig. 6. It is apparent that the increase of the fading parameter m decreases the outage probabilities dramatically. This can be explained by the fact
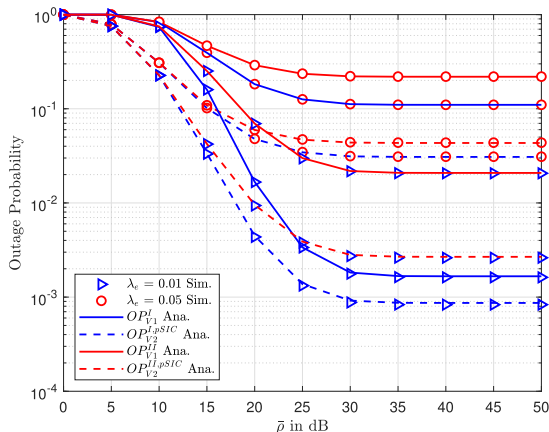
FIGURE 4. Outage performance of V_1 and V_2 versus $\bar{\rho}$ varying λ_e with $m = 2$, $\zeta = 0.01$, $\rho_I = 20$dB and $R = 1$ (BPCU).
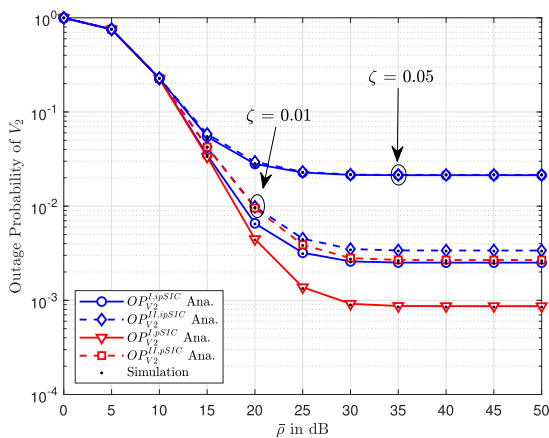

FIGURE 5. Outage performance of V_2 versus $\bar{\rho}$ varying ζ with $\lambda_e = 0.01$, $m = 1$, $\rho_I = 20$ (dB) and $R = 1$ (BPCU).
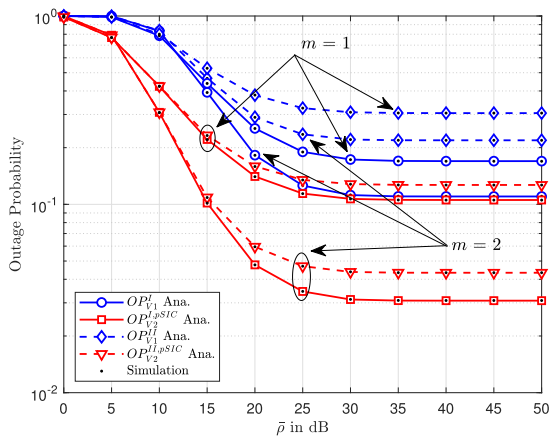

FIGURE 6. Outage performance of V_1 and V_2 versus $\bar{\rho}$ varying m with $\lambda_e = \zeta = 0.01$, $\rho_I = 20$ (dB) and $R = 1$(BPCU).

FIGURE 7. Outage performance of V_1 and V_2 versus α_1 varying $\bar{\rho}$ with $\lambda_e = 0.01$, $m = 1$ and $\rho_I = 20$ (dB).
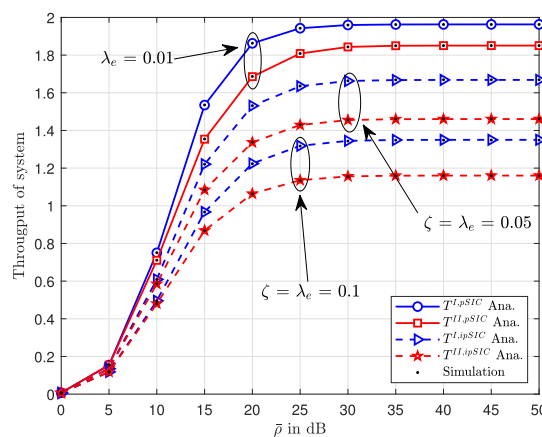
FIGURE 8. Throughput performance of system versus $\bar{\rho}$ with $\lambda_e = \zeta = (0.01, 0.05, 0.1)$, $m = 1$, and $R = 1$(BPCU).
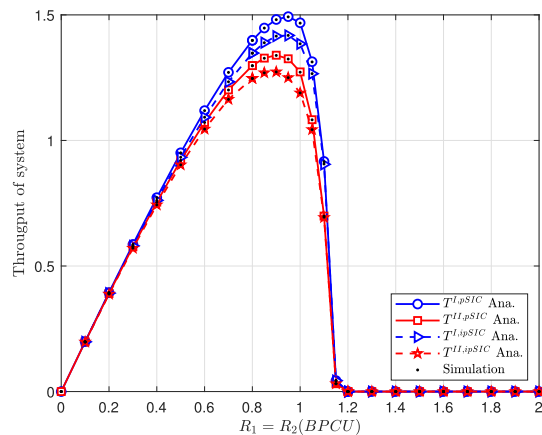
FIGURE 9. Throughput of system versus target rates with varying $\lambda_e = \zeta = 0.05$, $m = 1$, $\rho_I = 20$ (dB) and $R = 1$(BPCU).

that the existence of LOS for the vehicle with higher channel gain is able to dramatically decrease the outage probability.

The optimal outage behaviors of the two schemes are illustrated as result in Fig. 7. In particular, Fig. 7 indicates
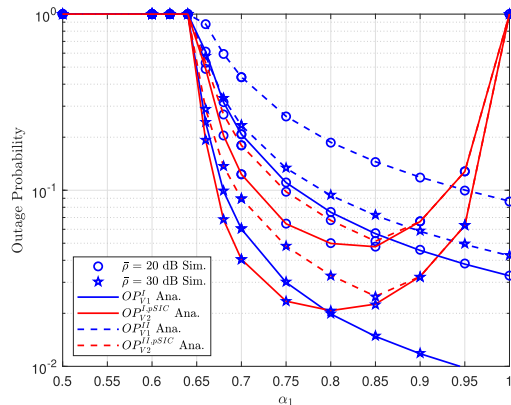
that increasing the power allocation factor α_1 can increase the optimal outage of vehicle V_2 while outage performance of vehicle V_1 improves significantly at high value of α_1, i.e. α_1 is approximate 1. The main reason for this is that a_1 makes a crucial impact on the achievable SINR while such SINR results in the different trends of outage behavior in two vehicles. For example, $\alpha_1 = 0.8$ provides the optimal outage performance for the vehicle V_2 at $\bar{\rho} = 30$ (dB).

Fig. 8 continues to confirm improvement of throughput of such system in the two schemes as SNR increases with different $\lambda_e = \zeta = (0.01, 0.05, 0.1)$. In Fig. 9, the impacts of the target rates R_1 and R_2 on the throughput performance of such system can be observed. The most important result is that at the maximum throughput can be obtained at $R_1, R_2 = 0.95$. Lower throughput can be seen at cases of imperfect SIC due to worse performance of the vehicle V_2. As previous results, performance gap among the two schemes exists in the range of target rates from 0 to 1.2.

VII. CONCLUSION

This paper proposes two schemes related to V2V transmission for CR-assisted NOMA-V2X, in which the vehicle cooperates with the nearby vehicle by exploiting two links for the mixture signal achieved, i.e. signal originated from both direct link associated with the BS and V2V link. The detailed performance analysis has been performed in terms of throughput and outage probability. Both closed-form and approximate expressions related to these metrics are derived precisely. The result have shown that a performance gap exists among two vehicles. It has also been found that the target rates and power allocation factors have the main impacts on these metrics for evaluating performance of SN, especially under impacts of both CSI imperfection and interference from the PN. Furthermore, the optimal power allocation factor can be indicated to obtain optimal outage performance for one of the two vehicles. Monte Carlo simulations have been included to verify the above performance analyses, and it confirms that CR-assisted NOMA-V2X works well with ability of V2V transmission.

APPENDIX A

With the help of (3), A_1 is given as,

$$
\begin{aligned}
&A_1 \\
&= 1 - \Pr\left(\gamma_{V_1 \to x_1} > \gamma_{th1}\right) \\
&= 1 - \underbrace{\Pr\left(\frac{\left|\hat{h}_1\right|^2 \alpha_1 \bar{\rho}_S}{\left|\hat{h}_1\right|^2 \alpha_2 \bar{\rho}_S + |e_1|^2 \bar{\rho}_S + \bar{\mu}} > \gamma_{th1}, \bar{\rho}_S < \frac{\rho_I}{|h_{SP}|^2}\right)}_{A_{1,1}} \\
&\quad - \underbrace{\Pr\left(\frac{\left|\hat{h}_2\right|^2 \alpha_1 \rho_I}{\left|\hat{h}_1\right|^2 \alpha_2 \rho_I + |e_1|^2 \rho_I + |h_{SP}|^2 \bar{\mu}} > \gamma_{th1}, \bar{\rho}_S > \frac{\rho_I}{|h_{SP}|^2}\right)}_{A_{1,2}},
\end{aligned}
$$
(73)

where $\bar{\rho}_S = \frac{\bar{P}_S}{N_0}$, $\bar{\rho}_{V_i} = \frac{\bar{P}_{V_i}}{N_0}$, $\bar{\rho} = \bar{\rho}_S = \bar{\rho}_{V_i}$ and $\rho_I = \frac{I_{th}}{N_0}$.

Then, the first term of (73), $A_{1,1}$ can be formulated as

$$
A_{1,1} = \underbrace{\Pr\left(\left|\hat{h}_1\right|^2 > \theta |e_1|^2 + \frac{\theta \bar{\mu}}{\bar{\rho}}\right)}_{A_{1,1,1}} \underbrace{\Pr\left(|h_{SP}|^2 < \frac{\rho_I}{\bar{\rho}}\right)}_{A_{1,1,2}},
$$
(74)

where $\theta = \frac{\gamma_{th1}}{\alpha_1 - \gamma_{th1}\alpha_2}$. Then, $A_{1,1,1}$ can be calculated as

$$
A_{1,1,1} = \int_0^\infty f_{|e_1|^2}(x) \bar{F}_{|\hat{h}_1|^2}\left(\theta x + \frac{\theta \bar{\mu}}{\bar{\rho}}\right) dx.
$$
(75)

With $\bar{F}(x) = 1 - F(x)$. By substituting (9) and (11) into (75) and we have

$$
\begin{aligned}
A_{1,1,1} = e^{-\frac{\theta \bar{\mu}}{\Omega_1 \bar{\rho}}} \sum_{i_1=0}^{m_1-1} \frac{\theta^{i_1}}{\Omega_1^{i_1} i_1!} \\
\times \int_0^\infty f_{|e_1|^2}(x)\left(x + \frac{\bar{\mu}}{\bar{\rho}}\right)^{i_1} e^{-\frac{\theta x}{\Omega_1}} dx.
\end{aligned}
$$
(76)

Based on [36, eq. 1.111,3.351.2] and after some algebra mathematical manipulations we get

$$
\begin{aligned}
A_{1,1,1} = \sum_{i_1=0}^{m_1-1} \sum_{n_1=0}^{i_1} \binom{m_{e_1} + n_1 - 1}{m_{e_1} - 1} \\
\times \frac{\theta^{i_1} C_1^{m_{e_1}} (H_1 \Omega_{SP} \bar{\rho})^{n_1 - i_1} e^{-\frac{\theta}{H_1 \Omega_{SP} \bar{\rho}}}}{(i_1 - n_1)! (\theta + C_1)^{m_{e_1} + n_1}},
\end{aligned}
$$
(77)

where $C_i = \frac{\Omega_i}{\Omega_{e_i}}$ and $H_i = \frac{\Omega_i}{\bar{\mu} \Omega_{SP}}$. With the help of (11) we can express $A_{1,1,2}$ as

$$
A_{1,1,2} = 1 - \frac{\Gamma\left(m_{SP}, \frac{\rho_I}{\Omega_{SP}\bar{\rho}}\right)}{\Gamma(m_{SP})}.
$$
(78)

Now, the second term of (73), $A_{1,2}$ an be shown as

$$
\begin{aligned}
A_{1,2} = \int_{\frac{\rho_I}{\bar{\rho}}}^\infty f_{|h_{SP}|^2}(z) \int_0^\infty f_{|e_1|^2}(x) \\
\times \bar{F}_{|\hat{h}_1|^2}\left(\theta x + \frac{\theta \bar{\mu}}{\rho_I} z\right) dx dz.
\end{aligned}
$$
(79)

Similarly, we can also get the following

$$
\begin{aligned}
A_{1,2} = \sum_{i_1=0}^{m_1-1} \sum_{k_1=0}^{i_1} \left(\frac{\bar{\mu}}{\rho_I}\right)^{k_1} \frac{\theta^{i_1}}{\Omega_1^{i_1} k_1! (i_1 - k_1)!} \\
\times \frac{\Omega_{SP}^{-m_{SP}} \Omega_{e_1}^{-m_{e_1}}}{(m_{SP} - 1)! (m_{e_1} - 1)!} \\
\times \int_{\frac{\rho_I}{\bar{\rho}}}^\infty z^{m_{SP} + k_1 - 1} e^{-\left(\frac{\theta \bar{\mu}}{\rho_I \Omega_1} + \frac{1}{\Omega_{SP}}\right) z} \\
\times \int_0^\infty x^{m_{e_1} + i_1 - k_1 - 1} e^{-\left(\frac{\theta}{\Omega_1} + \frac{1}{\Omega_{e_1}}\right) x} dx dz.
\end{aligned}
$$
(80)

With the help of [36, Eq.3.351.2 and Eq.3.351.3], $A_{1,2}$ can be written as

$$A_{1,2} = \sum_{i_1=0}^{m_1-1} \sum_{n_1=0}^{i_1} \sum_{k_1=0}^{m_{SP}+n_1-1} \binom{m_{e_1}+i_1-n_1-1}{m_{e_1}-1} \binom{m_{SP}+n_1-1}{m_{SP}-1}$$

$$\times \frac{C_1^{m_{e_1}} H_1^{m_{SP}-k_1} \rho_I^{m_{SP}} (\Omega_{SP}\bar{\rho})^{-k_1} \theta^{i_1} e^{-\frac{(\theta+\rho_I H_1)\bar{\mu}}{\bar{\rho}H_1\Omega_{SP}}}}{k_1! (\theta+C_1)^{m_{e_1}+i_1-n_1} (\theta+\rho_I H_1)^{m_{SP}+n_1-k_1}}. \tag{81}$$

Substituting (77) and (78) into (74), and by plugging the result and (81) into (73), the final result can be achieved.

It is end of the proof.

APPENDIX B

To start with, with the help of (4) and (5), the expected result of B_1 can be expressed as

$$\begin{aligned} B_1 &= \Pr\{\gamma_{V_2 \to x_1} > \gamma_{th1}, \gamma_{V_2 \to x_2} > \gamma_{th2}\} \\ &= \Pr\left\{\frac{|\hat{h}_2|^2 \alpha_1 \rho_S}{|\hat{h}_2|^2 \alpha_2 \rho_S + \rho_S |e_2|^2 + \bar{\mu}} > \gamma_{th1}, \frac{|\hat{h}_2|^2 \alpha_2 \rho_S}{\rho_S |e_2|^2 + \bar{\mu}} > \gamma_{th2}\right\} \\ &= \Pr\left\{|\hat{h}_2|^2 > \nu\left(|e_2|^2 + \frac{\bar{\mu}}{\rho_S}\right)\right\}, \end{aligned} \tag{82}$$

where $\beta_1 = \frac{\gamma_{th2}}{\alpha_2}$ and $\nu = \max(\beta_1, \theta)$. Moreover, it can be shown that B_1 as

$$B_1 = \underbrace{\Pr\left\{|\hat{h}_2|^2 > \nu|e_2|^2 + \frac{\nu\bar{\mu}}{\bar{\rho}}, \bar{\rho} < \frac{\rho_I}{|h_{SP}|^2}\right\}}_{B_{1,1}}$$

$$+ \underbrace{\Pr\left\{|\hat{h}_2|^2 > \nu|e_2|^2 + \frac{\nu\bar{\mu}|h_{SP}|^2}{\rho_I}, \bar{\rho} > \frac{\rho_I}{|h_{SP}|^2}\right\}}_{B_{1,2}}. \tag{83}$$

Next, based on (9) and (11) and after some manipulations, we can rewrite $B_{1,1}$ as

$$\begin{aligned} B_{1,1} &= \int_0^\infty f_{|e_2|^2}(x) \bar{F}_{|\hat{h}_2|^2}\left(\nu x + \frac{\nu\bar{\mu}}{\bar{\rho}}\right) dx \\ &= \sum_{i_2=0}^{m_2-1} \sum_{n_2=0}^{i_2} \binom{m_{e_2}+n_2-1}{m_{e_2}-1} \\ &\quad \times \frac{\nu^{i_2} C_2^{m_{e_2}} (H_2\Omega_{SP}\bar{\rho})^{n_2-i_2} e^{-\frac{\nu}{H_2\Omega_{SP}\bar{\rho}}}}{(i_2-n_2)! (\nu+C_2)^{m_{e_2}+n_2}}. \end{aligned} \tag{84}$$

Similarly, we can obtain $B_{1,2}$ as follows

$$B_{1,2} = \int_{\frac{\rho_I}{\bar{\rho}}}^\infty f_{|h_{SP}|^2}(z) \int_0^\infty f_{|e_2|^2}(x) \bar{F}_{|\hat{h}_2|^2}\left(\theta x + \frac{\theta\bar{\mu}}{\rho_I}z\right) dxdz$$

$$= \sum_{i_2=0}^{m_2-1} \sum_{n_2=0}^{i_2} \sum_{k_2=0}^{m_{SP}+n_2-1} \binom{m_{e_2}+i_2-n_2-1}{m_{e_2}-1} \binom{m_{SP}+n_2-1}{m_{SP}-1}$$

$$\times \frac{C_2^{m_{e_2}} H_2^{m_{SP}-k_2} \rho_I^{m_{SP}} (\Omega_{SP}\bar{\rho})^{-k_2} \theta^{i_2} e^{-\frac{\theta+\rho_I H_2}{\bar{\rho}H_2\Omega_{SP}}}}{k_2! (\theta+C_2)^{m_{e_2}+i_2-n_2} (\theta+\rho_I H_2)^{m_{SP}+n_2-k_2}}. \tag{85}$$

Finally, substituting (84) and (85) into (82) leads to (23). This completes the proof.

APPENDIX C

With the help of (4) and (34), $\bar{B}_1$ is written as

$$\begin{aligned} \bar{B}_1 &= \Pr\left\{|\hat{h}_2|^2 > \gamma_{th2}\bar{\alpha}|g_2|^2 + \beta_1\left(|e_2|^2 + \frac{\bar{\mu}}{\bar{\rho}}\right),\right. \\ &\quad \left. |\hat{h}_2|^2 > \theta\left(|e_2|^2 + \frac{\bar{\mu}}{\bar{\rho}}\right), |h_{SP}|^2 < \frac{\rho_I}{\bar{\rho}}\right\} \\ &\quad + \Pr\left\{|\hat{h}_2|^2 > \gamma_{th2}\bar{\alpha}|g_2|^2 + \beta_1\left(|e_2|^2 + \frac{\bar{\mu}|h_{SP}|^2}{\rho_I}\right),\right. \\ &\quad \left. |\hat{h}_2|^2 > \theta\left(|e_2|^2 + \frac{\bar{\mu}|h_{SP}|^2}{\rho_I}\right), |h_{SP}|^2 > \frac{\rho_I}{\bar{\rho}}\right\}, \tag{86} \end{aligned}$$

where $\bar{\alpha} = \frac{\bar{\alpha}_1}{\alpha_2}$. Then, for the case $\theta > \beta_1$, $\bar{B}_1$ is rewritten as in (87) shown at the bottom of the next page.

Further, J_1 can be changed to

$$\begin{aligned} J_1 &= F_{|h_{SP}|^2}\left(\frac{\rho_I}{\bar{\rho}}\right) \int_0^\infty f_{|e_2|^2}(x) \int_{\theta\left(x+\frac{\bar{\mu}}{\bar{\rho}}\right)}^\infty f_{|\hat{h}_2|^2}(y) \\ &\quad \times F_{|g_2|^2}\left(\frac{(\theta-\beta_1)}{\gamma_{th2}\bar{\alpha}}\left(x+\frac{\bar{\mu}}{\bar{\rho}}\right)\right) dydx \\ &= F_{|h_{SP}|^2}\left(\frac{\rho_I}{\bar{\rho}}\right)(J_{1,1} - J_{1,2}), \tag{88} \end{aligned}$$

where $J_{1,1}$ is expressed as

$$\begin{aligned} J_{1,1} &= \int_0^\infty f_{|e_2|^2}(x) \bar{F}_{|\hat{h}_2|^2}\left(\theta\left(x+\frac{\bar{\mu}}{\bar{\rho}}\right)\right) dx \\ &= \sum_{i_2=0}^{m_2-1} \sum_{p_2=0}^{i_2} \binom{m_{e_2}+i_2-p_2-1}{m_{e_2}-1} \\ &\quad \times \frac{C_2^{m_{e_2}} \theta^{i_2} (\theta+C_2)^{-m_{e_2}-i_2+p_2} e^{-\frac{\theta}{H_2\Omega_{SP}\bar{\rho}}}}{p_2! (H_2\Omega_{SP}\bar{\rho})^{p_2}}. \tag{89} \end{aligned}$$

Then, $J_{1,2}$ is shown as

$$\begin{aligned} J_{1,2} &= \int_0^\infty f_{|e_2|^2}(x) \bar{F}_{|\hat{h}_2|^2}\left(\theta\left(x+\frac{\bar{\mu}}{\bar{\rho}}\right)\right) \\ &\quad \times \bar{F}_{|g_2|^2}\left(\frac{(\theta-\beta_1)}{\gamma_{th2}\bar{\alpha}}\left(x+\frac{\bar{\mu}}{\bar{\rho}}\right)\right) dx \\ &= \sum_{i_2=0}^{m_2-1} \sum_{p_2=0}^{m_2-1} \sum_{n_2=0}^{i_2+p_2} \binom{m_{e_2}+i_2+p_2-n_2-1}{m_{e_2}-1} \binom{i_2+p_2}{i_2} \end{aligned}$$

$$\times \frac{C_2^{m_{e_2}} \theta^{p_2} (\theta - \beta_1)^{i_2} \bar{\zeta}^{m_{e_2}+p_2-n_2} e^{-\frac{\psi}{\zeta H_2 \Omega_{SP}\bar{\rho}}}}{n_2! (H_2 \Omega_{SP}\bar{\rho})^{n_2} (\psi + \bar{\zeta} C_2)^{m_{e_2}+i_2+p_2-n_2}}, \quad (90)$$

where $\bar{\zeta} = \zeta \gamma_{th2}\bar{\alpha}$ and $\psi = \bar{\zeta}\theta + \theta - \beta_1$. Similarly, J_2 can be easily calculated

$$J_2 = \sum_{i_2=0}^{m_2-1} \sum_{p_2=0}^{i_2} \sum_{n_2=0}^{m_2+i_2-p_2-1} \sum_{k_2=0}^{p_2+n_2} \binom{m_2+i_2-p_2-1}{m_2-1}$$
$$\times \binom{m_{e_2}+k_2-1}{m_{e_2}-1} \binom{p_2+n_2}{p_2} \frac{\beta_1^{p_2} C_2^{m_{e_2}} (\psi - \beta_1 \bar{\zeta})^{n_2}}{(p_2+n_2-k_2)!}$$
$$\times \frac{(\bar{\zeta}+1)^{-m_2-i_2+p_2} e^{-\frac{\psi}{\zeta H_2 \Omega_{SP}\bar{\rho}}} \left(1 - \frac{\Gamma(m_{SP}, \rho_I/\bar{\rho}\Omega_{SP})}{\Gamma(m_{SP})}\right)}{(\bar{\zeta} H_2 \Omega_{SP}\bar{\rho})^{p_2+n_2-k_2} (\psi + \bar{\zeta} C_2)^{m_{e_2}+k_2} \bar{\zeta}^{-m_{e_2}-i_2}}. \quad (91)$$

Next, J_3 is shown as

$$J_3 = \sum_{i_2=0}^{m_2-1} \sum_{p_2=0}^{i_2} \binom{m_{e_2}+i_2-p_2-1}{m_{e_2}-1} \frac{(H_2 \rho_I)^{m_{SP}}}{(\theta + H_2 \rho_I)^{m_{SP}+p_2}}$$
$$\times \frac{\theta^{i_2} C_2^{m_{e_2}} (\theta + C_2)^{p_2-m_{e_2}-i_2}}{p_2! \Gamma(m_{SP})} \Gamma\left(m_{SP}+p_2, \frac{\theta + \rho_I H_2}{H_2 \Omega_{SP}\bar{\rho}}\right)$$
$$- \sum_{i_2=0}^{m_2-1} \sum_{p_2=0}^{m_2-1} \sum_{n_2=0}^{i_2+p_2} \binom{m_{e_2}+i_2+p_2-n_2-1}{m_{e_2}-1} \binom{i_2+p_2}{i_2}$$
$$\times \frac{\theta^{i_2} C_2^{m_{e_2}} (\theta - \beta_1)^{p_2} \bar{\zeta}^{m_{SP}+m_{e_2}+i_2}}{n_2! \Gamma(m_{SP}) (\psi + \bar{\zeta} C_2)^{m_{e_2}+i_2+p_2-n_2}}$$
$$\times \frac{(H_2 \rho_I)^{m_{SP}}}{(\psi + \bar{\zeta} H_2 \rho_I)^{m_{SP}+n_2}} \Gamma\left(m_{SP}+n_2, \frac{\psi + \rho_I \bar{\zeta} H_2}{\bar{\zeta} H_2 \Omega_{SP}\bar{\rho}}\right). \quad (92)$$

Then, J_4 can be expressed as

$$J_4 = \sum_{i_2=0}^{m_2-1} \sum_{p_2=0}^{i_2} \sum_{n_2=0}^{m_2+i_2-p_2-1} \sum_{k_2=0}^{p_2+n_2} \binom{m_2+i_2-p_2-1}{m_2-1}$$
$$\times \binom{m_{e_2}+k_2-1}{m_{e_2}-1} \binom{p_2+n_2}{p_2} \frac{\beta_1^{p_2} (\psi - \bar{\zeta}\beta_1)^{n_2}}{(p_2+n_2-k_2)!}$$
$$\times \frac{C_2^{m_{e_2}} \bar{\zeta}^{m_{e_2}+i_2+m_{SP}} (\bar{\zeta}+1)^{p_2-m_2-i_2} (H_2 \rho_I)^{m_{SP}}}{(\psi + \bar{\zeta} C_2)^{m_{e_2}+k_2} (\psi + \bar{\zeta} H_2 \rho_I)^{m_{SP}+p_2+n_2-k_2}}$$
$$\times \Gamma\left(m_{SP}+p_2+n_2-k_2, \frac{\psi + \rho_I \bar{\zeta} H_2}{\bar{\zeta} H_2 \Omega_{SP}\bar{\rho}}\right). \quad (93)$$

Moreover, substituting (89) and (90) into (88) and the result with (91), (92) and (93), $\bar{B}_1$ can be obtained in this case. Next, for the case $\theta < \beta_1$, we can express $\bar{B}_1$ as

$$\bar{B}_1 = \underbrace{\int_0^{\frac{\rho_I}{\bar{\rho}}} f_{|h_{SP}|^2}(z) \int_0^{\infty} f_{|e_2|^2}(x) \int_0^{\infty} f_{|g_2|^2}(y)}_{J_5}$$
$$\bar{F}_{|\hat{h}_2|^2}\left(\gamma_{th2}\bar{\alpha}y + \beta_1\left(x + \frac{\bar{\mu}}{\bar{\rho}}\right)\right) dy dx dz$$
$$+ \underbrace{\int_{\frac{\rho_I}{\bar{\rho}}}^{\infty} f_{|h_{SP}|^2}(z) \int_0^{\infty} f_{|e_2|^2}(x) \int_0^{\infty} f_{|g_2|^2}(y)}_{J_6}$$
$$\bar{F}_{|\hat{h}_2|^2}\left(\gamma_{th2}\bar{\alpha}y + \beta_1\left(x + \frac{\bar{\mu}z}{\rho_I}\right)\right) dy dx dz. \quad (94)$$

$$\bar{B}_1 = \underbrace{\int_0^{\frac{\rho_I}{\bar{\rho}}} f_{|h_{SP}|^2}(z) \int_0^{\infty} f_{|e_2|^2}(x) \bar{F}_{|\hat{h}_2|^2}\left(\theta\left(x + \frac{\bar{\mu}}{\bar{\rho}}\right)\right) F_{|g_2|^2}\left(\frac{\theta - \beta_1}{\gamma_{th2}\bar{\alpha}}\left(x + \frac{\bar{\mu}}{\bar{\rho}}\right)\right) dx dz}_{J_1}$$

$$+ \underbrace{\int_0^{\frac{\rho_I}{\bar{\rho}}} f_{|h_{SP}|^2}(z) \int_0^{\infty} f_{|e_2|^2}(x) \int_{\frac{\theta-\beta_1}{\gamma_{th2}\bar{\alpha}}\left(x+\frac{\bar{\mu}}{\bar{\rho}}\right)}^{\infty} f_{|g_2|^2}(y) \bar{F}_{|\hat{h}_2|^2}\left(\gamma_{th2}\bar{\alpha}y + \beta_1\left(x + \frac{\bar{\mu}}{\bar{\rho}}\right)\right) dy dx dz}_{J_2}$$

$$+ \underbrace{\int_{\frac{\rho_I}{\bar{\rho}}}^{\infty} f_{|h_{SP}|^2}(z) \int_0^{\infty} f_{|e_2|^2}(x) \bar{F}_{|\hat{h}_2|^2}\left(\theta\left(x + \frac{\bar{\mu}z}{\rho_I}\right)\right) F_{|g_2|^2}\left(\frac{\theta - \beta_1}{\gamma_{th2}\bar{\alpha}}\left(x + \frac{\bar{\mu}z}{\rho_I}\right)\right) dx dz}_{J_3}$$

$$+ \underbrace{\int_{\frac{\rho_I}{\bar{\rho}}}^{\infty} f_{|h_{SP}|^2}(z) \int_0^{\infty} f_{|e_2|^2}(x) \int_{\frac{\theta-\beta_1}{\gamma_{th2}\bar{\alpha}}\left(x+\frac{\bar{\mu}z}{\rho_I}\right)}^{\infty} f_{|g_2|^2}(y) \bar{F}_{|\hat{h}_2|^2}\left(\gamma_{th2}\bar{\alpha}y + \beta_1\left(x + \frac{\bar{\mu}z}{\rho_I}\right)\right) dy dx dz}_{J_4}. \quad (87)$$

Similarly, J_5 can be expressed as

$$
\begin{aligned}
J_5 = \sum_{i_2=0}^{m_2-1} \sum_{p_2=0}^{i_2} \sum_{n_2=0}^{p_2} & \binom{m_2+i_2-p_2-1}{m_2-1} \\
\times & \binom{m_{e_2}+p_2-n_2-1}{m_{e_2}-1} \frac{\beta_1^{p_2} C_2^{m_{e_2}} e^{-\frac{\beta_1}{H_2 \Omega_{SP}\bar\rho}}}{(\beta_1+C_2)^{m_{e_2}+p_2-n_2}} \\
\times & \frac{\left(1-\frac{\Gamma(m_{SP}, \rho_I/\bar\rho\Omega_{SP})}{\Gamma(m_{SP})}\right)}{n_2! \bar\zeta^{-i_2+p_2}(\bar\zeta+1)^{m_2+i_2-p_2}(H_2\Omega_{SP}\bar\rho)^{n_2}}.
\end{aligned} \tag{95}
$$

Next, J_6 can be given by

$$
\begin{aligned}
J_6 = \sum_{i_2=0}^{m_2-1} \sum_{p_2=0}^{i_2} \sum_{n_2=0}^{p_2} & \binom{m_2+i_2-p_2-1}{m_2-1} \\
\times & \binom{m_{e_2}+p_2-n_2-1}{m_{e_2}-1} \frac{\beta_1^{p_2} C_2^{m_{e_2}}}{n_2!(\beta_1+C_2)^{m_{e_2}+p_2-n_2}} \\
\times & \frac{(\bar\zeta+1)^{-m_2-i_2+p_2} \bar\zeta^{i_2-p_2}}{(H_2\rho_I)^{n_2}\Gamma(m_{SP})}\left(\frac{\beta_1}{H_2\rho_I}+1\right)^{-m_{SP}-n_2} \\
\times & \Gamma\left(m_{SP}+n_2, \frac{\beta_1}{H_2\Omega_{SP}\bar\rho}+\frac{\rho_I}{\Omega_{SP}\bar\rho}\right).
\end{aligned} \tag{96}
$$

Finally, substituting (95) and (96) into (94), we can obtain (36).

The proof is completed.

APPENDIX D

First, (86) can be rewritten as

$$
\begin{aligned}
\bar B_1^{\bar\rho_S\to\infty} = \Pr \Bigg\{ & \left|\hat h_2\right|^2 > \gamma_{th2}\bar\alpha |g_2|^2 + \beta_1\left(|e_2|^2 + \frac{\bar\mu |h_{SP}|^2}{\rho_I}\right), \\
& \left|\hat h_2\right|^2 > \theta\left(|e_2|^2 + \frac{\bar\mu |h_{SP}|^2}{\rho_I}\right) \Bigg\}. \tag{97}
\end{aligned}
$$

Similarly, in case $\theta > \beta_1$ we have K_1 and K_2 are given respectively as

$$
\begin{aligned}
K_1 = \sum_{i_2=0}^{m_2-1} \sum_{p_2=0}^{i_2} & \binom{m_{e_2}+i_2-p_2-1}{m_{e_2}-1}\binom{m_{SP}+p_2-1}{m_{SP}-1} \\
\times & \frac{\theta^{i_2} C_2^{m_{e_2}} (H_2\rho_I)^{m_{SP}}(\theta+C_2)^{-m_{e_2}-i_2+p_2}}{(\theta+H_2\rho_I)^{m_{SP}+p_2}} \\
- \sum_{i_2=0}^{m_2-1} \sum_{p_2=0}^{m_2-1} \sum_{n_2=0}^{i_2+p_2} & \binom{m_{e_2}+i_2+p_2-n_2-1}{m_{e_2}-1}\binom{m_{SP}+n_2-1}{m_{SP}-1} \\
\times & \binom{i_2+p_2}{i_2} \frac{\theta^{i_2} C_2^{m_{e_2}} (\theta-\beta_1)^{p_2}(H_2\rho_I)^{m_{SP}} \bar\zeta^{m_{e_2}+m_{SP}+i_2}}{(\psi+\bar\zeta C_2)^{m_{e_2}+i_2+p_2-n_2}(\psi+\bar\zeta H_2\rho_I)^{m_{SP}+n_2}},
\end{aligned} \tag{98}
$$

and

$$
\begin{aligned}
K_2 = \sum_{i_2=0}^{m_2-1} \sum_{p_2=0}^{i_2} \sum_{n_2=0}^{m_2+i_2-p_2-1} \sum_{k_2=0}^{p_2+n_2} & \binom{m_{e_2}+p_2+n_2-k_2-1}{m_{e_2}-1}
\end{aligned}
$$

$$
\begin{aligned}
\times & \binom{m_2+i_2-p_2-1}{m_2-1}\binom{m_{SP}+k_2-1}{m_{SP}-1}\binom{p_2+n_2}{n_2} \\
\times & \frac{\beta_1^{p_2} C_2^{m_{e_2}} (\psi-\bar\zeta\beta_1)^{n_2}(\bar\zeta+1)^{-m_2-i_2+p_2} \bar\zeta^{m_{SP}+m_{e_2}+i_2}}{(\rho_I H_2)^{-m_{SP}}(\psi+\bar\zeta C_2)^{m_{e_2}+p_2+n_2-k_2}(\psi+\bar\zeta H_2\rho_I)^{m_{SP}+k_2}}.
\end{aligned} \tag{99}
$$

Moreover, it can computed $\bar K$ in case $\theta > \beta_1$ as

$$
\begin{aligned}
\bar K = \sum_{i_2=0}^{m_2-1} \sum_{p_2=0}^{i_2} \sum_{n_2=0}^{p_2} & \binom{m_2+i_2-p_2-1}{m_2-1}\binom{m_{e_2}+p_2-n_2-1}{m_{e_2}-1} \\
\times & \binom{m_{SP}+n_2-1}{m_{SP}-1} \frac{\beta_1^{p_2} C_2^{m_{e_2}}}{(\beta_1+C_2)^{m_{e_2}+p_2-n_2}} \\
\times & \frac{\bar\zeta^{i_2-p_2}(H_2\rho_I)^{m_{SP}}}{(\beta_1+H_2\rho_I)^{m_{SP}+n_2}(\bar\zeta+1)^{m_2+i_2-p_2}}. \tag{100}
\end{aligned}
$$

Finally, it leads to achieve the final result.

REFERENCES

[1] T. Sahin, M. Klugel, C. Zhou, and W. Kellerer, "Virtual cells for 5G V2X communications," *IEEE Commun. Standards Mag.*, vol. 2, no. 1, pp. 22–28, Mar. 2018.

[2] R. Molina-Masegosa and J. Gozalvez, "LTE-V for sidelink 5G V2X vehicular communications: A new 5G technology for short-range vehicle-to-everything communications," *IEEE Veh. Technol. Mag.*, vol. 12, no. 4, pp. 30–39, Dec. 2017.

[3] H. Ullah, N. Gopalakrishnan Nair, A. Moore, C. Nugent, P. Muschamp, and M. Cuevas, "5G communication: An overview of Vehicle-to-everything, drones, and healthcare use-cases," *IEEE Access*, vol. 7, pp. 37251–37268, 2019.

[4] (Apr. 2013). *Scenarios, Requirements and KPIs for 5G Mobile and Wireless System. METIS ICT-317669 METIS/D1.1, METIS Deliverable D1.1.* [Online]. Available: https://www.metis2020.com/documents/deliverables/

[5] B. W. Khoueiry and M. R. Soleymani, "An efficient NOMA V2X communication scheme in the Internet of vehicles," in *Proc. VTC-Spring*, Sydney, NSW, Australia, Jun. 2017, pp. 1–7.

[6] X. Li, J. Li, Y. Liu, Z. Ding, and A. Nallanathan, "Residual transceiver hardware impairments on cooperative NOMA networks," *IEEE Trans. Wireless Commun.*, vol. 19, no. 1, pp. 680–695, Jan. 2020.

[7] X. Li, M. Liu, C. Deng, P. T. Mathiopoulos, Z. Ding, and Y. Liu, "Full-duplex cooperative NOMA relaying systems with I/Q imbalance and imperfect SIC," *IEEE Wireless Commun. Lett.*, vol. 9, no. 1, pp. 17–20, Jan. 2020.

[8] T.-L. Nguyen and D.-T. Do, "Exploiting impacts of intercell interference on SWIPT-assisted non-orthogonal multiple access," *Wireless Commun. Mobile Comput.*, vol. 2018, pp. 2525492-1–2525492-12, Nov. 2018.

[9] D.-T. Do, A.-T. Le, and B. M. Lee, "NOMA in cooperative underlay cognitive radio networks under imperfect SIC," *IEEE Access*, vol. 8, pp. 86180–86195, 2020.

[10] X. Li, Q. Wang, H. Peng, H. Zhang, D.-T. Do, K. M. Rabie, R. Kharel, and C. C. Cavalcante, "A unified framework for HS-UAV NOMA networks: Performance analysis and location optimization," *IEEE Access*, vol. 8, pp. 13329–13340, 2020.

[11] D.-T. Do and M.-S. Van Nguyen, "Device-to-device transmission modes in NOMA network with and without wireless power transfer," *Comput. Commun.*, vol. 139, pp. 67–77, May 2019.

[12] D.-T. Do and A.-T. Le, "NOMA based cognitive relaying: Transceiver hardware impairments, relay selection policies and outage performance comparison," *Comput. Commun.*, vol. 146, pp. 144–154, Oct. 2019.

[13] B. Di, L. Song, Y. Li, and Z. Han, "V2X meets NOMA: Non-orthogonal multiple access for 5G-enabled vehicular networks," *IEEE Wireless Commun.*, vol. 24, no. 6, pp. 14–21, Dec. 2017.

[14] G. Liu, Z. Wang, J. Hu, Z. Ding, and P. Fan, "Cooperative NOMA broadcasting/multicasting for low-latency and high-reliability 5G cellular V2X communications," *IEEE Internet Things J.*, vol. 6, no. 5, pp. 7828–7838, Oct. 2019.

[15] D. Zhang, Y. Liu, L. Dai, A. K. Bashir, A. Nallanathan, and B. Shim, "Performance analysis of FD-NOMA-Based decentralized V2X systems," *IEEE Trans. Commun.*, vol. 67, no. 7, pp. 5024–5036, Jul. 2019.

[16] H. Xiao, Y. Chen, S. Ouyang, and A. T. Chronopoulos, "Power control for clustering car-following V2X communication system with non-orthogonal multiple access," *IEEE Access*, vol. 7, pp. 68160–68171, 2019.

[17] I. Kakalou, K. E. Psannis, P. Krawiec, and R. Badea, "Cognitive radio network and network service chaining toward 5G: Challenges and requirements," *IEEE Commun. Mag.*, vol. 55, no. 11, pp. 145–151, Nov. 2017.

[18] G. Im and J. H. Lee, "Outage probability for cooperative NOMA systems with imperfect SIC in cognitive radio networks," *IEEE Commun. Lett.*, vol. 23, no. 4, pp. 692–695, Apr. 2019.

[19] B. Li, X. Qi, K. Huang, Z. Fei, F. Zhou, and R. Q. Hu, "Security-reliability tradeoff analysis for cooperative NOMA in cognitive radio networks," *IEEE Trans. Commun.*, vol. 67, no. 1, pp. 83–96, Jan. 2019.

[20] D. Wang and S. Men, "Secure energy efficiency for NOMA based cognitive radio networks with nonlinear energy harvesting," *IEEE Access*, vol. 6, pp. 62707–62716, 2018.

[21] Z. Xiang, W. Yang, G. Pan, Y. Cai, and Y. Song, "Physical layer security in cognitive radio inspired NOMA network," *IEEE J. Sel. Topics Signal Process.*, vol. 13, no. 3, pp. 700–714, Jun. 2019.

[22] W. Xu, R. Qiu, and X.-Q. Jiang, "Resource allocation in heterogeneous cognitive radio network with non-orthogonal multiple access," *IEEE Access*, vol. 7, pp. 57488–57499, 2019.

[23] Y. Liu, Z. Ding, M. Elkashlan, and J. Yuan, "Nonorthogonal multiple access in large-scale underlay cognitive radio networks," *IEEE Trans. Veh. Technol.*, vol. 65, no. 12, pp. 10152–10157, Dec. 2016.

[24] L. Lv, J. Chen, Q. Ni, and Z. Ding, "Design of cooperative non-orthogonal multicast cognitive multiple access for 5G systems: User scheduling and performance analysis," *IEEE Trans. Commun.*, vol. 65, no. 6, pp. 2641–2656, Jun. 2017.

[25] L. Lv, Q. Ni, Z. Ding, and J. Chen, "Application of non-orthogonal multiple access in cooperative spectrum-sharing networks over Nakagami-*m* fading channels," *IEEE Trans. Veh. Technol.*, vol. 66, no. 6, pp. 5506–5511, Jun. 2017.

[26] T.-L. Nguyen and D.-T. Do, "Power allocation schemes for wireless powered NOMA systems with imperfect CSI: An application in multiple antenna-based relay," *Int. J. Commun. Syst.*, vol. 31, no. 15, p. e3789, Oct. 2018.

[27] X. Li, J. Li, and L. Li, "Performance analysis of impaired SWIPT NOMA relaying networks over imperfect Weibull channels," *IEEE Syst. J.*, vol. 14, no. 1, pp. 669–672, Mar. 2020, doi: 10.1109/JSYST.2019.2919654.

[28] F. Fang, H. Zhang, J. Cheng, S. Roy, and C. M. Victor Leung, "Joint user scheduling and power allocation optimization for energy-efficient NOMA systems with imperfect CSI," *IEEE J. Sel. Areas Commun.*, vol. 35, no. 12, pp. 2874–2875, Dec. 2017.

[29] K. Eshteiwi, G. Kaddoum, K. Ben Fredj, E. Soujeri, and F. Gagnon, "Performance analysis of full-duplex vehicle relay-based selection in dense multi-lane highways," *IEEE Access*, vol. 7, pp. 61581–61595, 2019.

[30] K. Eshteiwi, G. Kaddoum, B. Selim, and F. Gagnon, "Impact of co-channel interference and vehicles as obstacles on full-duplex V2V cooperative wireless network," *IEEE Trans. Veh. Technol.*, early access, May 8, 2020, doi: 10.1109/TVT.2020.2993508.

[31] S. Arzykulov, T. A. Tsiftsis, G. Nauryzbayev, and M. Abdallah, "Outage performance of cooperative underlay CR-NOMA with imperfect CSI," *IEEE Commun. Lett.*, vol. 23, no. 1, pp. 176–179, Jan. 2019.

[32] J.-B. Kim, I.-H. Lee, and J. Lee, "Capacity scaling for D2D aided cooperative relaying systems using NOMA," *IEEE Wireless Commun. Lett.*, vol. 7, no. 1, pp. 42–45, Feb. 2018.

[33] N. Madani and S. Sodagari, "Performance analysis of non-orthogonal multiple access with underlaid device-to-device communications," *IEEE Access*, vol. 6, pp. 39820–39826, 2018.

[34] S. M. A. Kazmi, N. H. Tran, T. M. Ho, A. Manzoor, D. Niyato, and C. S. Hong, "Coordinated device-to-device communication with non-orthogonal multiple access in future wireless cellular networks," *IEEE Access*, vol. 6, pp. 39860–39875, 2018.

[35] A. Tassi, M. Egan, R. J. Piechocki, and A. Nix, "Modeling and design of millimeter-wave networks for highway vehicular communication," *IEEE Trans. Veh. Technol.*, vol. 66, no. 12, pp. 10676–10691, Dec. 2017.

[36] D. Zwillinger, *Table of Integrals, Series, and Products*, 7th ed. New York, NY, USA: Academic, 2007.

[37] Y. Zhang, J. Ge, and E. Serpedin, "Performance analysis of a 5G energy-constrained downlink relaying network with non-orthogonal multiple access," *IEEE Trans. Wireless Commun.*, vol. 16, no. 12, pp. 8333–8346, Dec. 2017.

[38] Y. Zhang, J. Ge, and E. Serpedin, "Performance analysis of non-orthogonal multiple access for downlink networks with antenna selection over Nakagami-*m* fading channels," *IEEE Trans. Veh. Technol.*, vol. 66, no. 11, pp. 10590–10594, Nov. 2017.

DINH-THUAN DO (Senior Member, IEEE) received the B.S., M.Eng., and Ph.D. degrees in communications engineering from Viet Nam National University (VNU-HCM), in 2003, 2007, and 2013, respectively. He was a Visiting Ph.D. Student with the Communications Engineering Institute, National Tsing Hua University, Taiwan, from 2009 to 2010. Prior to joining Ton Duc Thang University, he was a Senior Engineer with the VinaPhone Mobile Network, from 2003 to 2009. He has published over 65 SCI/SCIE journal articles, one sole author book and five book chapters. His research interests include signal processing in wireless communications networks, cooperative communications, non-orthogonal multiple access, full-duplex transmission, and energy harvesting. He was a recipient of the Golden Globe Award from Vietnam Ministry of Science and Technology, in 2015 (Top 10 excellent young scientists nationwide). He is currently serving as an Associate Editor in six journals, in which main journals are *EURASIP Journal on Wireless Communications and Networking*, *Computer Communications* (Elservier), and the *KSII Transactions on Internet and Information Systems*.

TU ANH LE was born in Lam Dong, Vietnam. He is currently pursuing the master's degree in communication and information system in the field of wireless communications. He is currently a Research Assistant with the WICOM Laboratory which was led by Dr. Thuan. He has authored or coauthored over five technical articles published in peer-reviewed international journals. His research interests include the wireless channel modeling, NOMA, cognitive radio, and MIMO.

TU N. NGUYEN (Senior Member IEEE) received the Ph.D. degree in electronic engineering from the National Kaohsiung University of Science and Technology (formerly, National Kaohsiung University of Applied Sciences), Kaohsiung, Taiwan, in 2016. He was a Postdoctoral Associate with the Department of Computer Science and Engineering, University of Minnesota-Twin Cities, in 2017. Prior to joining the University of Minnesota, he joined the Missouri University of Science and Technology as a Postdoctoral Researcher with the Intelligent Systems Center, in 2016. He is currently an Assistant Professor with the Department of Computer Science, Purdue University Fort Wayne, Fort Wayne, IN, USA. His research interests include design and analysis of algorithms, network science, cyber-physical systems, and cybersecurity. He has been an Associate Editor for IEEE ACCESS and the *EURASIP Journal on Wireless Communications and Networking*, since 2017. He has been on the Editorial Board of the *Cybersecurity Journal*, *Internet Technology Letters*, since 2017, the *International Journal of Vehicle Information and Communication Systems*, since 2017, the *International Journal of Intelligent Systems Design and Computing*, since 2017, and *IET Wireless Sensor Systems* since 2017. He was a TPC Co-Chair for the NAFOSTED Conference on Information and Computer Science (NICS) 2019, SoftCOM (25th) and the EAI International Conference on Context-Aware Systems and Applications (ICCASA) 2017, the Publicity Chair for International Conference on Awareness Science and Technology (iCAST) 2017 and BigDataSecurity 2017, and a Track Chair for ACT 2017. He was also a Technical Program Committee Member for more than 70 premium conferences in the areas of network and communication, such as INFOCOM, Globecom, ICC, and RFID.

XINGWANG LI (Senior Member, IEEE) received the B.Sc. degree from Henan Polytechnic University, in 2007, the M.Sc. degree from the University of Electronic Science and Technology of China, in 2010, and the Ph.D. degree from the Beijing University of Posts and Telecommunications in 2015. From 2010 to 2012, he was working as an Engineer with Comba Telecom Ltd., Guangzhou, China. He spent one year from 2017 to 2018 as a Visiting Scholar with Queen's University Belfast, Belfast, U.K. He is also a Visiting Scholar with the State Key Laboratory of Networking and Switching Technology, Beijing University of Posts and Telecommunications, from 2016 to 2018. He is currently an Associate Professor with the School of Physics and Electronic Information Engineering, Henan Polytechnic University, Jiaozuo, China. His research interests include MIMO communication, cooperative communication, hardware constrained communication, non-orthogonal multiple access, physical layer security, unmanned aerial vehicles, and the Internet-of-Things. He is an Editor on the Editorial Board of IEEE Access, *Computer Communications*, and the *KSII Transactions on Internet and Information Systems*. He has served as many TPC members, such as the IEEE/CIC International Conference on Communications in China (ICCC'2019) and the IEEE Global Communications Conference 2018 (Globecom'18).

KHALED M. RABIE (Senior Member, IEEE) received the B.S. degree (Hons.) from Tripoli University, Libya, in 2008, the M.Sc. degree and the Ph.D. degree in electrical and electronic engineering from the University of Manchester, Manchester, U.K., in 2010 and 2015, respectively. He joined the Manchester Metropolitan University (MMU), U.K., where he is currently an Assistant Professor with the Department of Engineering. He has published more than 90 articles in prestigious journals and international conferences, and serves regularly on the Technical Program Committee of several major IEEE conferences such as GLOBECOM, ICC, VTC, and so on. His primary research focuses on various aspects of the next-generation wireless communication systems. He is also a Fellow of the U.K. Higher Education Academy (FHEA). He has received numerous awards over the past few years in recognition of his research contributions including the Best Student Paper Award at the IEEE ISPLC, TX, USA, 2015, the MMU Outstanding Knowledge Exchange Project Award of 2016 and the IEEE Access Editor of the Month Award for August 2019. He serves as an Associate Editor of IEEE Access, an Area Editor of *Physical Communication* (Elsevier), and an Executive Editor of the *Transactions on Emerging Telecommunications Technologies* (Wiley).

● ● ●